Target Vehicle Selection Algorithm Based on Lane-changing Intention of Preceding Vehicle for ACC

Jun Yao
College of Automotive Engineering, Jilin University
Guoying Chen
State Key Laboratory of Automotive Simulation and Control, Jilin University
Zhenhai Gao (gaozh@jlu.edu.cn)
Jilin University

Review

Keywords: Lane-changing intention, target vehicle selection, support vector machine, adaptive cruise control

Posted Date: January 26th, 2021

DOI: https://doi.org/10.21203/rs.3.rs-89924/v2

Title page

Target Vehicle Selection Algorithm Based on Lane-changing Intention of Preceding Vehicle for ACC

Jun Yao, born in 1995, is currently a PhD student at *College of Automotive Engineering, Jilin University, Changchun, China*. He received his bachelor degree from *Jilin University, China*, in July 2020. His research interests include vehicle dynamics and control, and autonomous vehicles.
E-mail: yaojun1995@139.com

Guo-Ying Chen, born in 1984, is currently an associate professor at *Jilin University, China*. He received his PhD degree from *Jilin University, China*, in 2012. His research interests include control-by-wire vehicle control and autonomous vehicles.
E-mail: cgy-011@163.com

Zhen-Hai Gao, is a professor at in *Jilin University, China*. Dr. Gao received his Ph.D. degree in automotive engineering from *Jilin University*, 2000. He was a foreign researcher of the *University of Tokyo*. In recent years, his research has been focused on connected & automated vehicles, driver behavior analysis, advanced driver assistance system, and human-machine interface.
E-mail: gaozh@jlu.edu.cn

Corresponding author：Zhen-Hai Gao　E-mail：gaozh@jlu.edu.cn

ORIGINAL ARTICLE

Target Vehicle Selection Algorithm Based on Lane-changing Intention of Preceding Vehicle for ACC

Jun Yao[1] • Guo-Ying Chen[2] • Zhen-Hai Gao[2]

Received June xx, 201x; revised February xx, 201x; accepted March xx, 201x

Abstract: In order to improve the ride comfort and safety of the traditional adaptive cruise control (ACC) system when the preceding vehicle changes lanes, this paper proposes a target vehicle selection algorithm based on the prediction of the lane-changing intention of the preceding vehicle. First, NGSIM dataset is used to train a lane-changing intention prediction algorithm based on sliding window SVM, and the lane-changing intent of the preceding vehicle in the current lane can be identified by lateral position offset. Secondly, according to the lane-changing intention and the collision threat of the preceding vehicle, the target vehicle selection algorithm is studied under three different conditions: safe lane-changing condition, dangerous lane-changing condition, and lane-changing cancellation condition. Finally, the effectiveness of the algorithm proposed in this paper is verified in the co-simulation platform. The simulation results show that the target vehicle selection algorithm proposed in this paper can ensure the smooth transfer of the target vehicle and effectively reduce the longitudinal acceleration fluctuation of the subject vehicle when the preceding vehicle changes lanes safely or cancels the lane change. In the case of a dangerous lane change, the target vehicle selection algorithm proposed in this paper can respond to the dangerous lane change in advance compared with the target vehicle selection method of the traditional ACC system, which can effectively avoid collisions and improve the safety of the subject vehicle.

Keywords: Lane-changing intention, target vehicle selection, support vector machine, adaptive cruise control

✉ Zhen-Hai Gao
gaozh@jlu.edu.cn

[1] College of Automotive Engineering, Jilin University, Changchun 130022, China

[2] State Key Laboratory of Automotive Simulation and Control, Jilin University, Changchun 130022, China

1 Introduction

With the increasingly serious traffic congestion, adaptive cruise control (ACC), as the key technology of advanced driver assistance systems (ADAS), has been widely concerned, and gradually entered the lives of ordinary people. According to statistical reports, lane changes are the main cause in car crashes [1-4]. When the preceding vehicle changes lanes, traditional ACC system just declares the target vehicle (vehicle that the subject vehicle follows) as the closest one currently in the subject vehicle's lane, which cannot comprehensively consider the lane-changing vehicle. Under this condition, there will be large fluctuations in longitudinal acceleration which greatly reduces ride comfort, and may even cause collision risks [5-6]. In order to prevent this, a key enabling technology is a reliable lane-changing intention prediction technology, which can recognize that the preceding vehicle has the intention to change lanes before it crosses the lane line. This allows the subject vehicle to respond in advance to the preceding vehicle's lane-changing action, thereby reducing acceleration's fluctuation and avoiding collisions.

The most relevant prediction methods of preceding vehicle's lane-changing intention in literature can be roughly divided into four categories, i.e., the fuzzy logic-based method, the support vector machine (SVM)-based method, the hidden Markov model (HMM)-based method and the deep learning-based method.

The fuzzy logic-based method uses relative motion information between the subject vehicle and the preceding vehicle as the input variable. And through fuzzy logic, the lane-changing intention of the preceding vehicle can be

obtained which can effectively realize human control strategy and experience. Seungwuk Moon et al. [7-8] introduce a lane-changing intention predictor based on fuzzy logic, which uses the relative lateral distance and relative lateral speed between the preceding vehicle and the subject vehicle as the input, and uses the fuzzy rules to determine the lane-changing probability of the preceding vehicle. It is considered that the vehicles with smaller lateral relative distance and larger lateral relative speed have the higher probability to change lane. The fuzzy rules in the literature are mainly based on the fitting curve of relative speed and relative distance under the preceding vehicle's cut-in condition. However, the fuzzy logic controller largely depends on human experience, and cannot objectively identify lane-changing intention.

The SVM-based method is to select the appropriate feature vector according to relative motion information, and obtain the best parameters of SVM through training, to predict the lane-changing intention of the preceding vehicle. Ma Guocheng et al. [9-10] uses data collected from actual traffic environment as training samples, to identify cut-in maneuver of adjacent lane vehicles based on fuzzy support vector machines (FSVM). In order to improve the training accuracy of cut-in identifier , a fuzzy membership coefficient is introduced for each sample in solving FSVM , and a grid optimization is conducted on the parameters of FSVM. Hanwool Woo et al. [11] define the feature vector as consisting of the distance from the centerline, the lateral velocity, and the potential feature. The potential feature is to characterize the possibility of lane-changing by analyzing the location relationship between the preceding vehicle and its surrounding vehicles. By adding potential feature, the proposed SVM algorithm can eliminate the false prediction caused by zigzag driving.

The HMM-based method is mainly based on the observed state information of the preceding vehicle to identify the independent and invisible lane-changing intention. Ma Shijie established a mixed Gaussian-Hidden Markov model to describe the lane changing behavior of adjacent vehicles. The driver's decision states are segmented and described by the model parameters [12]. And the lateral distance between the preceding vehicle and the center of the host vehicle are used to characterize the changes of decision states. On the basis of the literature [12], Zhang Kexin divided the lane-changing process into the safe lane changing process and the dangerous lane changing process based on the collision risk [13]. According to the characteristics of lane keeping and lane change, and the characteristics of safe lane change and dangerous lane change, the HMM-based lane-changing identification method of sliding time window is designed respectively, and the driving state of each time window is judged in turn. Dejan Mitrovic proposed a simple and reliable method for identifying driving events using HMM [14]. By collecting real-vehicle experimental data and manually selecting observation sequences for training and verification, each observation sequence is classified into specific types of events, and the HMM model parameters of each driving event are trained respectively. The observation sequence from the training set is evaluated by multiple models. By comparing the probability of the observation sequence calculated by each HMM model, the event corresponding to the highest HMM model is selected as the estimation result.

The deep learning-based method is to predict the preceding vehicle's lane-changing intention or driving trajectory through the neural network. This method requires a huge dataset for parameter training, to obtain better prediction results. Zhang Hailun et al. [15] uses the speech recognition framework as an example to map the behavior of the preceding vehicle (lane change, keep lane) to different speech words. Since the motion information of the preceding vehicle and the surrounding vehicles are both continuous and time-varying, and words of different sizes correspond to different driving styles during lane changes. The speech recognition model can be well applied to the recognition of the lane-changing behavior of the preceding vehicle. Seungje Yoon et al. [16] calculates the likelihood of multiple target lanes and trajectories of surrounding vehicles through a radial basis function network (RBFN). The RBFN prediction algorithm uses the classification distribution and the future trajectory to estimate the probability of each lane becoming the driver's target lane in parallel, and converts the RBFN into a probability model which considers uncertainty. Donghan Lee et al. [17] proposes a lane-changing intention recognizer based on Convolutional Neural Network (CNN). This method transforms real-world driving data to a simplified bird's-eye view, which enables a CNN-based inference approach with low computation cost and robustness to noisy input.

Most of the current literature is to predict the lane-changing intention of the preceding vehicle in the adjacent lane (as shown in Figure 1), but the prediction result of the lane-changing intention of the preceding vehicle in the current lane (as shown in Figure 2) will also have an impact on the longitudinal acceleration of the subject vehicle. For example, when the preceding vehicle in the current lane changes lanes, if a low-speed commercial vehicle or a stationary object appears in front

of the current lane, the subject vehicle will also face acceleration fluctuations or even the danger of collision. Therefore, this paper studies the lane-changing intention prediction algorithm for both the preceding vehicle in adjacent lane and the preceding vehicle in current lane. When most of the literature uses SVM to identify the intention of lane-changing of the preceding vehicle, they only select the certain feature vector and kernel function of SVM, and do not explain the reasons for the selection of those SVM parameters. This paper compares the prediction accuracy of different types of SVM, selects the radial basis function (RBF) as the kernel function and analyzes the influence of different sliding window sizes on the prediction accuracy. Moreover, most of the literature only studies the successful lane-change of the preceding vehicle, without considering the failure or cancellation of the preceding vehicle's lane change. This paper studies the selection of the target vehicle when the preceding vehicle fails to change lanes.

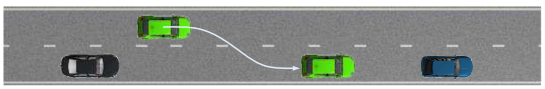

Figure 1 Schematic diagram of lane change of the preceding vehicle in adjacent lane

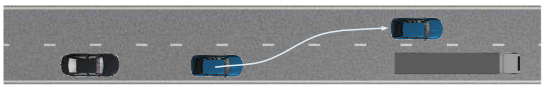

Figure 2 Schematic diagram of lane change of the preceding vehicle in current lane

The remaining of this paper is structured as follows: Section 2 illustrates the system architecture. Section 3 introduces the lane-changing intention prediction algorithm. Section 4 introduces the target vehicle selection algorithm. Section 5 studies the longitudinal motion control algorithm. Section 6 evaluates the proposed algorithm in simulation and Section 7 concludes the paper.

2 System Architecture

The overall framework proposed in this paper is shown in Figure 3. It is mainly divided into three parts: the lane-changing intention prediction, the target vehicle selection, and the longitudinal motion control. First, the lane-changing intention of the preceding vehicle is mainly predicted by the sliding window SVM algorithm. This paper uses the NGSIM dataset to train the parameters of the SVM, and determine the size of the sliding window. The lane-changing intention of the preceding vehicle in current lane is predicted by lateral relative distance offset. The next step is to select the target vehicle. The target vehicle selection is to determine the target vehicle under three different conditions: safe lane-changing condition, dangerous lane-changing condition, and lane-changing cancellation condition. Longitudinal motion control is to generate the actuator control quantity based on the status information of the target vehicle. The actuator control quantity is composed of two parts: the feedforward control quantity and the feedback control quantity.

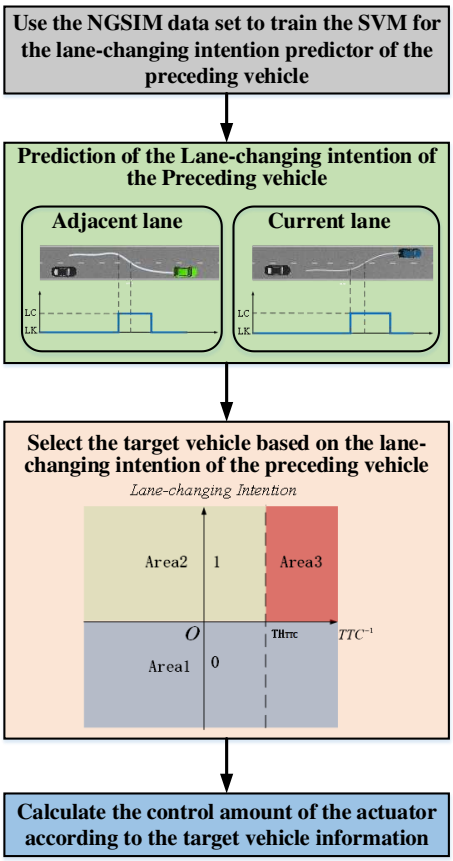

Figure 3 The overall framework of longitudinal control algorithm based on prediction of the lane-changing intention of the preceding vehicle

3 Lane-changing intention prediction algorithm based on sliding window SVM

When the preceding vehicle changes lanes, the traditional ACC system cannot comprehensively consider the preceding vehicle in current lane and the lane-changing vehicle. There will be large fluctuations in longitudinal acceleration under this condition, which greatly reduces the ride comfort and may even cause collision danger. In

order to avoid the violent fluctuation of the longitudinal acceleration caused by the jump of the target vehicle, the sliding window SVM algorithm is adapted to identify the lane-changing intention of the preceding vehicle.

3.1 NGSIM dataset preprocessing

This paper intends to use the public dataset recorded by the Next Generation Simulation (NGSIM) program initiated by the Federal Highway Administration in 2002 to train the sliding window SVM [18]. This project uses high-definition cameras installed above the road to record the vehicle driving data, and uses video processing software to obtain the vehicle trajectory data in a period of 0.1s. The lane-changing vehicle data on US 101 highway in the NGSIM dataset is used to train the lane-changing intention prediction SVM in this paper. The study aera schematic and camera coverage of NGSIM US 101 highway data is shown in Figure 4.

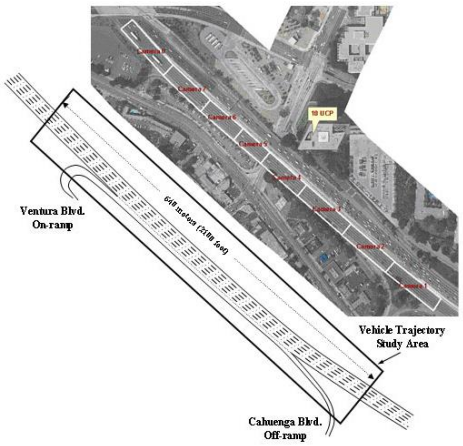

Figure 4 Study aera schematic and camera coverage of NGSIM US 101 highway data

After simply filtering, 6100 individual vehicle driving data can be obtained. Since this paper studies the free lane-changing behavior of passenger cars, reasonable lane-changing vehicle data need to meet the following constraints:

1) Since this paper is to study the free lane changing of cars, it is necessary to restrict the types of vehicles to 2-cars.

2) Lane 7 and lane 8 of US 101 highway are both ramps, lane 6 is the auxiliary lane of the ramp entrance, lane 1 is the leftmost lane, and lane 5 is the rightmost lane, adjacent to lane 6. In order to avoid the influence of the forced lane-changing behavior data made by vehicles entering and exiting the ramp, the lane-changing vehicle data used in this paper excludes the vehicle trajectory containing lanes 6, 7, and 8 in its driving lane ID, and ensures that the lane ID in the vehicle trajectory data changes.

3) In order to prevent the change of the vehicle lane ID caused by the vehicle driving near the lane line all the time, this paper compares the deviation of the lateral position between the start and the end of the lane change to ensure this deviation is greater than 2.75m.

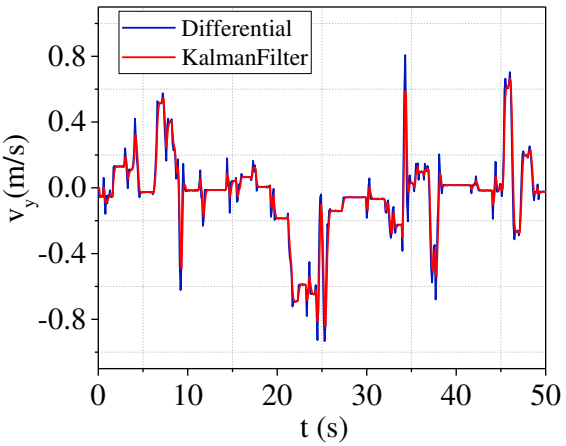

Figure 5 Kalman filtering result of relative lateral velocity

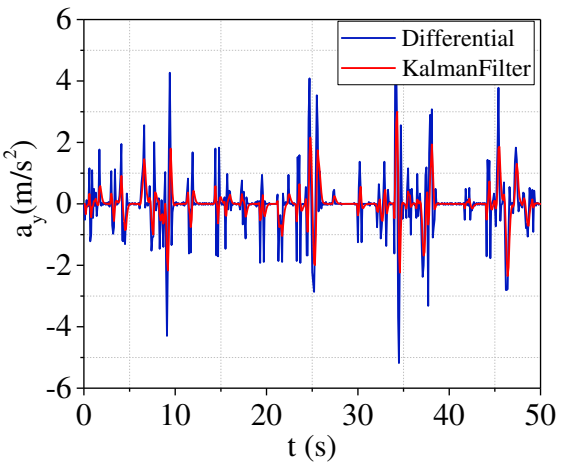

Figure 6 Kalman filtering result of relative lateral acceleration

Through artificial selection, 184 reasonable lane-changing vehicle trajectories can be obtained. Since the subject vehicle can only obtain the relative position and relative speed information of the preceding vehicle through the vehicle sensors, it is necessary to calculate the relative lateral distance and relative lateral speed of the preceding vehicle relative to the road centerline of the target lane. By subtracting the local coordinate of the target lane centerline from the local coordinate of the lane-changing vehicle, the relative lateral distance of the lane-changing vehicle relative to the centerline of the target lane can be obtained. In order to reduce the influence of NGSIM dataset

measurement error, Kalman filter is used to calculate the relative lateral velocity v_y and relative lateral acceleration a_y of the preceding vehicle relative to the road centerline of the target lane. The estimated relative lateral velocity v_y and relative lateral acceleration a_y are shown in Figure 5 and Figure 6. The relative lateral velocity calculated by Kalman filter is basically the same as that obtained by local coordinate Y's difference in original NGSIM dataset, but the spike is effectively suppressed. Comparing the relative lateral acceleration calculated by Kalman filter with the acceleration data obtained by velocity difference, the relative lateral acceleration calculated by Kalman filter can well restrain the fluctuation caused by the difference.

3.2 SVM algorithm design

3.2.1 SVM algorithm

SVM is a very widely used algorithm in machine learning. It is mainly to find a suitable hyperplane in a multi-dimensional space as a classification plane to maximize the minimum spacing of positive and negative samples in the sample space. The samples that reach the minimum spacing are called support vectors. For the linear inseparable case, the support vector machine can use the kernel function to transform the nonlinear classification situation into the linearly separable situation in the high-dimensional sample space [19-21]. The commonly used kernel functions are: polynomial kernel function, Gaussian kernel function, etc.

Suppose the classification function is

$$h_{\bar{w},b}(\bar{x}) = g\left(\bar{w}^T \bar{x} + b\right) \tag{1}$$

where $g(z) = \begin{cases} 1 \ if \ z \geq 0 \\ 0 \ if \ z < 0 \end{cases}$, and $\bar{w}, b$ are the training parameters, $\bar{x}$ is the feature vector.

In the prediction model of the lane-changing intention of the preceding vehicle, $h_{\bar{w},b}(\bar{x}) = 1$ means the preceding vehicle has the intention to change lanes, and $h_{\bar{w},b}(\bar{x}) = 0$ means that the preceding vehicle has no intention to change lanes and will continue to drive in the original lane. The optimization goal of the support vector machine is to maximize the geometric margins between positive and negative samples. The definition of geometric margin $\gamma^{(i)}$ is as follows, and γ are the smallest one:

$$\begin{gathered} \gamma^{(i)} = y^{(i)}\left(\left(\frac{\bar{w}}{\| \bar{w} \|}\right)^T \bar{x}^{(i)} + \frac{b}{\| \bar{w} \|}\right) \\ \gamma = \min_{i=1,2...m} \gamma^{(i)} \end{gathered} \tag{2}$$

where m represents the number of samples in the training set.

The original optimization problem of support vector machine is as follows:

$$\begin{aligned} \max_{\gamma,\bar{w},b} \quad & \gamma \\ \text{s.t.} \quad & y^{(i)}\left(\bar{w}^T \bar{x}^{(i)} + b\right) \geq \gamma, \quad i = 1,\ldots,m \\ & \| \bar{w} \| = 1 \end{aligned} \tag{3}$$

Since there is a non-convex constraint $\| \bar{w} \| = 1$ in the original optimization problem, the original problem is very difficult to solve. So, it needs to be transformed into a convex optimization problem:

$$\begin{aligned} & \min_{\gamma,w,b} \frac{1}{2} \| \bar{w} \|^2 \\ & \text{s.t. } y^{(i)}\left(\bar{w}^T \bar{x}^{(i)} + b\right) \geq 1, \quad i = 1,\ldots,m \end{aligned} \tag{4}$$

Through Lagrange duality, the above convex optimization problem can be transformed into a quadratic programming problem:

$$\begin{aligned} \max_{\lambda} W(\lambda) = & \sum_{i=1}^{m} \lambda_i - \frac{1}{2} \sum_{i,j=1}^{m} y^{(i)} y^{(j)} \lambda_i \lambda_j \left\langle \bar{x}^{(i)}, \bar{x}^{(j)} \right\rangle \\ & \text{s.t. } \lambda_i \geq 0, \quad i = 1,\ldots,m \\ & \sum_{i=1}^{m} \lambda_i y^{(i)} = 0 \end{aligned} \tag{5}$$

where $\left\langle \bar{x}^{(i)}, \bar{x}^{(j)} \right\rangle$ represents the kernel function value of $\bar{x}^{(i)}, \bar{x}^{(j)}$, and λ represents the Lagrange multiplier.

3.2.2 SVM feature vector selection

The feature vector selected in the literature [10] include: longitudinal relative distance between the subject vehicle and the preceding vehicle, lateral relative distance, longitudinal relative speed, lateral relative speed, longitudinal relative acceleration, lateral relative acceleration, and subject vehicle speed, which is shown in Figure 7. However, the training samples are limited and cannot cover the all feature vector that may appear during using SVM, for example: the current speed of the subject vehicle never appears in the training sample, or the current longitudinal relative distance, longitudinal relative speed, and longitudinal relative acceleration exceed the range of the feature vector in the training sample. In the above cases, the accuracy of lane-changing intention prediction obtained by SVM is very low. Literature [11] selects the lateral relative distance, lateral relative speed, and Potential Feature of the preceding vehicle relative to the centerline

of the driving lane of the subject vehicle as feature vector. Potential feature, which analyzes the position relationship between the preceding vehicle and its surrounding traffic vehicles, represents the lane-changing risk degree of the preceding vehicle. This feature is added to improve the situation of false prediction when the preceding vehicle is zigzag driving in its original lane. However, millimeter-wave radar and cameras, as the main sensor systems of ADAS, cannot obtain comprehensive and accurate motion state information of traffic vehicles around the preceding vehicle. In addition, this paper holds that the preceding vehicle's zigzag driving in the original lane does not necessarily mean that it is in the process of lane-changing failure. It may also be due to the inexperienced driving of novice drivers, or the target vehicle is in the target lane adjustment stage after lane change. The potential feature cannot be used to solve all zigzag driving misjudgments.

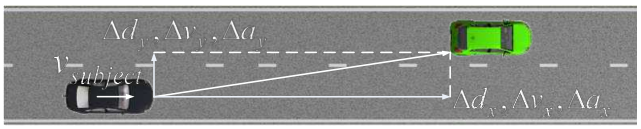

Figure 7 Schematic diagram of feature vector selected in [10]

The feature vector selected in this paper include: the lateral relative distance d_y and lateral relative speed v_y of the preceding vehicle relative to the centerline of the driving lane of the subject vehicle. When only using the relative motion information at the current moment as the feature vector, a short-term misjudgment will often occur due to the jump of the motion state. However, the lane-changing intention prediction of the preceding vehicle at the current moment is often related to the relative motion information in the previous several cycles. Therefore, this paper takes the relative motion information of the preceding vehicle relative to the centerline of the driving lane of the subject vehicle in the previous k cycles as the feature vector. The feature vector $\bar{x}_t$ at time t can be expressed as follows.

$$\bar{x}_t = \left[\bar{D}_y, \bar{V}_y \right] \tag{6}$$

$$\bar{D}_y = \left[d_{y,t-(k-1)}, d_{y,t-(k-2)}, \mathrm{L}\ d_{y,t} \right] \tag{7}$$

$$\bar{V}_y = \left[v_{y,t-(k-1)}, v_{y,t-(k-2)}, \mathrm{L}\ v_{y,t} \right] \tag{8}$$

where $\bar{D}_y$ is the feature of the lateral relative distance, and $\bar{V}_y$ is the feature of the lateral relative speed relative to the centerline of the driving lane of the subject vehicle. Selecting the relative motion information of the preceding vehicle relative to the centerline of the driving lane of the subject vehicle as the feature vector, instead of the relative motion information of the preceding vehicle relative to the subject vehicle, on the one hand, can avoid the influence of the lateral movement of the subject vehicle on the lane-changing intention prediction. On the other hand, it is very convenient to convert the relative lateral distance into d coordinate under *Frenet* coordinate when driving in curves[22-23].

Figure 8 Schematic diagram of feature vector selected in this paper

3.2.3 SVM parameter training

In order to solve the impact of different feature units, the z-score normalization is used to standardize the features. The mean value of each feature after processed is 0, and the standard deviation is 1. Before the SVM parameter training, NGSIM dataset samples are divided into training set and test set samples according to the ratio of 7:3. The number of samples of training set and test set are 10080 and 4273 respectively. SVM with different parameters is trained by using training set samples, and the SVM prediction accuracy is tested by test set samples. At the same time, this paper uses cross validation method to divide the training set data into N copies (N=5 in this paper). In each training process, N-1 of them is selected for training, and the remaining one is used as the validation set. Through n-training, a group of parameters with the highest accuracy of the validation set is selected as the final training result. The flow chart of the SVM parameter training is shown in Figure 9.

Linear function, quadratic function, cubic function, and radial basis function (RBF) are selected as the kernel function to train SVM. At the same time, in order to determine the size of the sliding window, this paper trains the SVM with four different kernel functions in the window size range of 0s~5s with an interval of 0.2s. The training result is shown in Figure 10.

From Figure 10(d), when the sliding window size is 0.4s, the test set accuracy of the linear kernel function SVM reaches the maximum value of 0.676. Since quadratic kernel function, cubic kernel function and RBF kernel function can map sample features to higher space and achieve nonlinear classification, the validation set accuracy and test set accuracy of the above three kernel function

SVM are improved in different degrees compared with linear kernel function SVM. The RBF kernel function SVM has the most obvious improvement effect. The test set accuracy of the RBF kernel function SVM can reach 0.935 when the sliding window is 2.2s. Therefore, this paper chooses the RBF kernel function SVM to predict the lane-changing intention of the preceding vehicle.

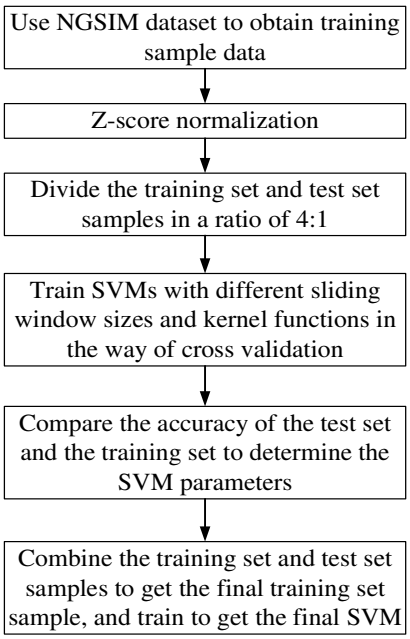

Figure 9 The flow chart of the SVM parameter training

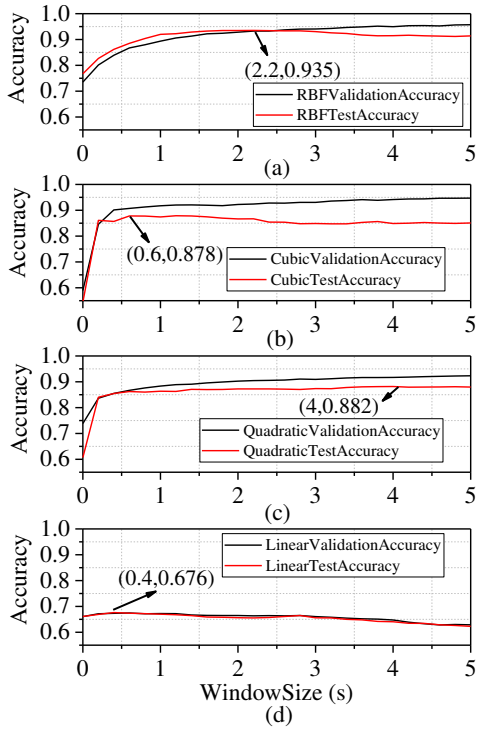

Figure 10 Validation accuracy and test accuracy of SVM with four different kernel functions in the sliding window size range of 0s~5s with an interval of 0.2s

Comparing the accuracy of test set and verification set, it can be found that the test set accuracy of the above three kernel function SVM is lower than the validation set accuracy to some extent. When the size of sliding window increases, the number of features increases, and overfitting occurred during SVM training. As the size of the sliding window increases, the validation set accuracy can be continuously improved. But when the sliding window size exceeds a certain range, the test set prediction accuracy decreases as the size of the time window increases (the RBF kernel function SVM is particularly obvious), that is, the size of sliding window is not the longer, the better.

As shown in Figure 10(a), when the sliding window size is 2.2s, the test set accuracy of the RBF kernel function SVM reaches the highest. Therefore, this paper selects the RBF kernel function SVM with a sliding window size of 2.2s to predict the lane-changing intention of the preceding vehicle. After determining the SVM kernel function and sliding window size, this paper combines the test set samples and the training set samples to form a new training set sample, and trains to obtain the final lane-changing intention prediction SVM. The parameters of the final SVM for the lane-changing intention prediction of the preceding vehicle are shown in Table 1.

Table 1 The parameters of the final SVM for the lane-changing intention prediction of the preceding vehicle

Parameters	Value
SVM kernel function	RBF
Sliding window size	2.2s
KernelScale	8.5
BoxConstraint	20.5

where KernelScale is the parameter γ of the RBF, where RBF has the following forms: $K\left(\bar{x}^{(i)},\bar{x}^{(j)}\right)=e^{-\gamma\left\|\bar{x}^{(i)}-\bar{x}^{(j)}\right\|}$, and BoxConstraint is a positive value that controls the penalty imposed on observations with large residuals[24].

3.3 Prediction results of lane-changing intention of the preceding vehicle in adjacent lane

The prediction results of the lane-changing intention of the preceding vehicle in the adjacent lane is shown in Figure 11. It can be seen from Figure 11(a) that the preceding vehicle is zigzag driving in the original lane within 4.3s-7s after the start of the simulation. And the lane change starts at 10.5s, and ends at the 15s. The overall lane changing time is 4.5s. It can be seen from Figure 11(b) that the

lane-changing intention prediction SVM based on sliding window designed in this paper (denoted as SVM_2.2s) predicts that the preceding vehicle has lane-changing intention at the 11.9s. From Figure 11(a), the preceding vehicle passes through the lane line of the lane where the subject vehicle is located at 13.2s, which means the lane-changing intention prediction SVM based on sliding window can identify the lane-changing intention of the preceding vehicle 1.3s in advance. Figure 11(c) shows the prediction results of SVM that only uses the motion state information at the current moment as the feature vector (denoted as SVM_0s). There are short-term misjudgments in the 4.9s and 6s. Since SVM_0s only uses the motion state information at the current moment as the feature vector, it is easy to make misjudgments when the motion state jumps during the zigzag driving. The lane-changing intention prediction SVM designed in this paper uses the motion state information of the entire sliding window (the window size is 2.2s), so it can deal with the disturb of motion state changes caused by the zigzag driving.

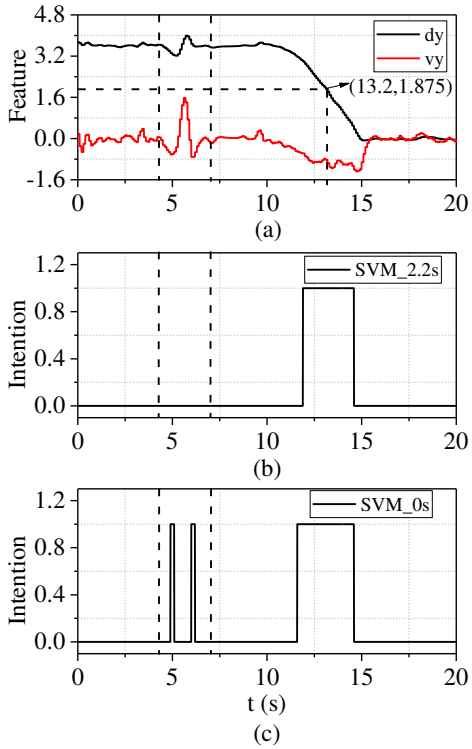

Figure 11 The prediction results of the lane-changing intention of the preceding vehicle in the adjacent lane: (a) features of SVM; (b) the lane-changing intention prediction by SVM_2.2s; (c) the lane-changing intention prediction by SVM_0s

Compared with the traditional ACC target vehicle selection algorithm, the advance time of lane-changing intention prediction output by SVM is related to many factors, such as the initial relative lateral distance when the preceding vehicle begins to change lanes, the overall lane-changing time, etc. Figure 12 shows the prediction results of lane-changing intention of the preceding vehicle under three different overall lane-changing times, with overall lane-changing time of 3.1s, 5.0s and 6.9s respectively. The lane-changing intention prediction SVM designed in this paper can identify the lane-changing intention of the preceding vehicle 0.9s, 1.7s, and 2.3s in advance, compared with the traditional ACC target vehicle selection algorithm. As the overall lane-changing time increases, the advance time increases accordingly. Therefore, the advance time cannot be used as the only criterion to judge the quality of lane-changing intention prediction SVM.

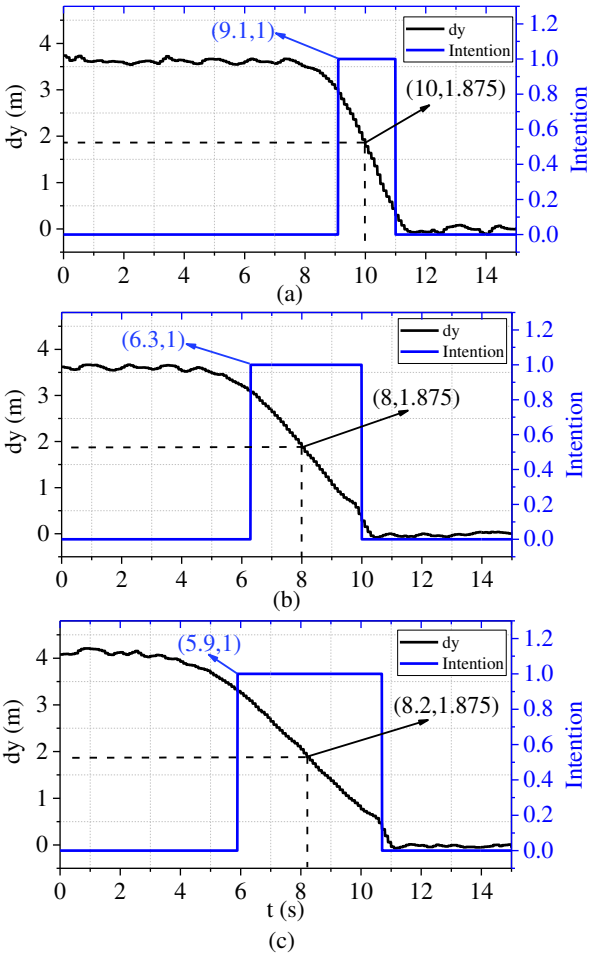

Figure 12 The prediction results of lane-changing intention of the preceding vehicle under three different overall lane-changing times: (a) the overall lane-changing time is 3.1s; (b) the overall lane-changing time is 5.0s; (c) the overall lane-changing time is 6.9s

Table 2 Advance time for different overall lane-changing time

Overall lane-changing time	Advance time

Overall lane-changing time	Advance time
3.1s	0.9s
5.0s	1.7s
6.9s	2.3s

3.4 Prediction results of lane-changing intention of the preceding vehicle in current lane

When the preceding vehicle in the current lane changes lanes, if a low-speed vehicle or a stationary object appears in front of the current lane, the subject vehicle will also face acceleration fluctuations or even the danger of collision. Therefore, it is meaningful to identify the lane-changing intention of the preceding vehicle in the current lane. However, since the lane-changing intention prediction SVM designed in this paper uses the lateral relative distance and lateral relative speed of the preceding vehicle relative to the centerline of the target lane as the feature vector, it cannot be directly applied to the prediction of the lane-changing intention of the preceding vehicle in the current lane. To solve this problem, the lateral relative distance of the preceding vehicle in the current lane is offset left and right respectively. The offset distance is one lane width, as shown in Figure 13.

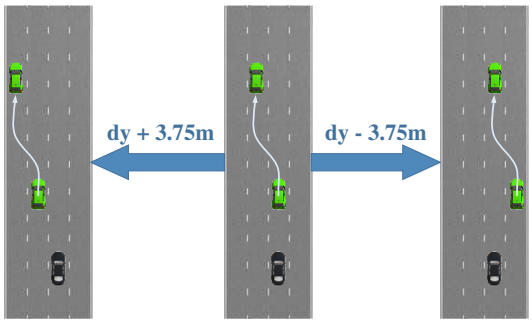

Figure 13 Schematic diagram of relative lateral distance offset

The offset of lateral relative distance does not affect the magnitude of lateral relative velocity. By inputting the offset lateral relative distance and lateral relative speed into the lane-changing intention prediction SVM as the feature vector, the lane-changing intention of the preceding vehicle in the current lane, with the left and right adjacent lanes as the target lane, can be identified. If the lane width is shifted to the left, the target lane of the preceding vehicle can be changed from the right adjacent lane to the current lane, and the right lane-changing intention of the vehicle in the current lane can be identified by using the lane-changing intention prediction SVM. In the same way, if the lane width is shifted to the right, the target lane of the preceding vehicle can be changed from the left adjacent lane to the current lane, and the left lane-changing intention of the vehicle in the current lane can be identified. The prediction results of the lane-changing intention of the preceding vehicle in the current lane is shown in Figure 14.

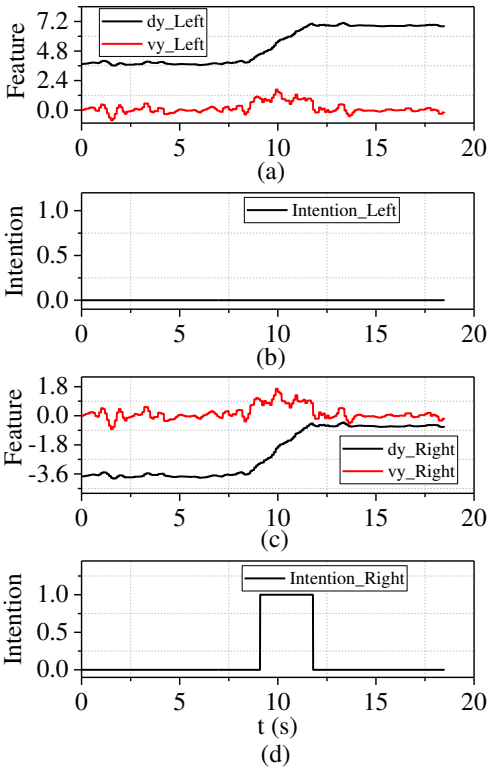

Figure 14 The prediction results of the lane-changing intention of the preceding vehicle in the current lane: (a) features of the left lane-changing intention prediction SVM; (b) the left lane-changing intention prediction; (c) features of the right lane-changing intention prediction SVM; (d) the right lane-changing intention prediction

Since the relative lateral distance after shifting to the left by one lane width ranges from 3.7m to 7.5m, the prediction result of right lane-changing intention of the preceding vehicle is always zero, which means that the preceding vehicle does not have the right lane-changing intention. However, when the lateral relative distance offset to the right and the lateral relative velocity are taken as the feature vector, the left lane-changing intention of the preceding vehicle can be identified by SVM at 10.6s. Compared with the traditional ACC target vehicle selection algorithm, the lane-changing intention of the preceding vehicle in the current lane can be identified 1s in advance.

4 Target vehicle selection based on the prediction of the lane-changing intention of the preceding vehicle

This paper does not consider the situation that both the preceding vehicle in the current lane and the preceding vehicle in the adjacent lane change lanes at the same time. Only the situation that one of them changes lane is considered in this paper, and we take the lane change of the preceding vehicle in the adjacent lane as an example to illustrate the target vehicle selection process.

In order to select the target vehicle, it is necessary to calculate the collision threat of each target. The collision threat is represented by TTC^{-1} in this paper [25-26]. TTC^{-1} can be calculated as follows:

$$TTC^{-1} = -\frac{v_x}{d_x} \tag{9}$$

where d_x is the longitudinal relative distance, v_x is the longitudinal relative speed between the preceding vehicle and the subject vehicle, which equals the difference between the longitudinal speed of subject vehicle $v_{subject}$ and that of the preceding vehicle $v_{preceding}$.

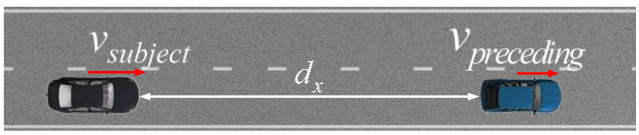

Figure 15 Schematic diagram of the longitudinal relative distance and the longitudinal relative speed

When TTC^{-1} is greater than zero, it means that the preceding vehicle is approaching, and there is a risk of collision. The collision threat increases with the increase of TTC^{-1}. When TTC^{-1} is less than zero, it means that the preceding vehicle is far away from the subject vehicle and there is no collision risk.

According to the lane-changing intention (denoted as *Intention*) and the collision threat of each target, the targets in the adjacent lane can be classified into the three types, which are represented by *DriveStatue* [7], as shown in Figure 16.

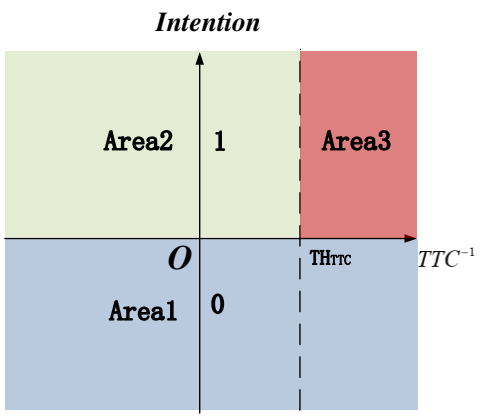

Figure 16 Schematic diagram of *DriveStatue* of effective target

The target in the Aera1 means: the preceding vehicle has no lane-changing intention (*Intention*=0). In this case, the *DriveStaue* is equal to 0. The target in the Aera2 means: the preceding vehicle has lane-changing intention and there is no collision risk (*Intention*=1, $TTC^{-1} < Th_{TTC}$). In this case, the *DriveStaue* is equal to 1. The target in the Aera3 means: the preceding vehicle has lane-changing intention and there is a risk of collision (Intention=1, $TTC^{-1} \geqslant Th_{TTC}$). In this case, the *DriveStaue* is equal to 2.

Because there may be multiple vehicles in the adjacent lane ahead having lane-changing intention, it is necessary to select the "most threatening" target from them, as the target vehicle in the adjacent lane. Firstly, according to the *DriveStatue* of the targets in the adjacent lane, we can get the driving status with the highest priority at the current time as the representative *DriveStatue*, denoted as *RDS*:

$$RDS = max\{DriveStatue_i\}, i = 1,2,3\ldots n \tag{10}$$

where *n* is the number of targets in the adjacent lane.

Among the targets whose *DriveStatue* is *RDS* in the adjacent lane, the one with the smallest longitudinal relative distance from the subjected vehicle is selected as the target vehicle in the adjacent lane. According to different *RDS* value, the fusion method of the target vehicle in the adjacent lane and the target closest to the subject vehicle in the current lane (the target vehicle obtained by the traditional ACC target vehicle selection algorithm, denoted as the target vehicle in the current lane) is also different. $d_{x,inlane}$ and $v_{x,inlane}$ represent the longitudinal relative distance and the longitudinal relative speed between the target vehicle in the current lane and the subject vehicle, $d_{x,\text{adjacent lane}}$ and $v_{x,\text{adjacent lane}}$ represent the longitudinal relative distance and the longitudinal relative speed between the target vehicle in the adjacent lane and the subject vehicle.

Case 1: *RDS* =0, there is no vehicle in the adjacent lanes having the lane-changing intention, so the target vehicle in the current lane can be directly selected as the target vehicle.

$$d_{x,main} = d_{x,inlane} \tag{11}$$

$$v_{x,main} = v_{x,inlane} \tag{12}$$

Case 2: *RDS*=1, the target vehicle in the adjacent lane has the lane-changing intention and there is no risk of collision, which means the target vehicle in the adjacent lane

changes lanes safely. In this case, the target vehicle selection needs to fuse the target vehicle in the current lane with the target vehicle in the adjacent lane:

$$d_{x,main} = \alpha d_{x,inlane} + (1-\alpha) d_{x,\text{adjacent lane}} \tag{13}$$

$$v_{x,main} = \alpha v_{x,inlane} + (1-\alpha) v_{x,\text{adjacent lane}} \tag{14}$$

$$\alpha = \min\left\{ \frac{\left\| |d_{y,Init}| - |d_{y,\text{adjacentlane}| \right\|}{\left\| d_{\text{y,}Init} \right| - 0.875|}, 1 \right\} \tag{15}$$

where $d_{y,Init}$ is the lateral relative distance of the target vehicle in adjacent lane relative to the center line of the lane where the subject vehicle is located when the target vehicle in adjacent lane is first detected having the lane-changing intention, and $d_{y,\text{adjacentlane}}$ is the lateral relative distance of the target vehicle in adjacent lane relative to the center line of the lane where the subject vehicle is located.

During the lane-changing process of the target vehicle in adjacent lane, $d_{y,\text{adjacentlane}}$ will change from $d_{y,Init}$ to 0.875m (When the lateral relative distance of the target in the adjacent lane is less than 0.875m, this target can be considered as the target in the current lane.), and α will smoothly transfer from 0 to 1.

Case 3: *RDS* =2, the target vehicle in the adjacent lane has the lane-changing intention and there is a risk of collision, which means the target vehicle in the adjacent lane changes lanes dangerously. In this case, the primary goal is the safety of the subject vehicle. So, the target vehicle in the adjacent lane can be directly selected as the target vehicle.

$$d_{x,main} = d_{x,adjacentlane} \tag{16}$$

$$v_{x,main} = v_{x,adjacentlane} \tag{17}$$

As shown in Figure 17, in some cases, the preceding vehicle will stop changing lanes and return to its original lane. When it is detected that the preceding vehicle cancels the lane change, if the target vehicle is directly changed back to the target vehicle in the current lane, the longitudinal acceleration of the subject vehicle will inevitably fluctuate due to the jump of the target vehicle.

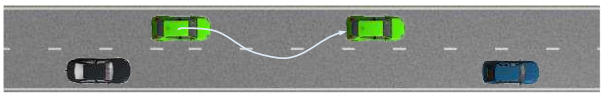

Figure 17 Schematic diagram of the preceding vehicle's lane-changing cancellation

When the lane-changing intention of the target vehicle in the adjacent vehicle changes from 1 to 0, and $d_{y,\text{adjacentlane}}$ is greater than 0.875m, it can be determined that the target vehicle in the adjacent vehicle cancels the lane change. Under lane-changing cancellation condition, the target vehicle state is calculated as follows:

$$d_{x,main} = \beta d_{x,inlane} + (1-\beta) d_{x,\text{adjacent lane}} \tag{18}$$

$$v_{x,main} = \beta v_{x,inlane} + (1-\beta) v_{x,\text{adjacent lane}} \tag{19}$$

$$\beta = \alpha_{cancel} \cdot \max\left\{ \frac{2.875 - |d_{y,\text{adjacentlane}}|}{|2.875 - |d_{y,\text{cancel}}||}, 0 \right\} \tag{20}$$

where $d_{y,\text{cancel}}$ is the lateral relative distance of the target vehicle in adjacent lane relative to the center line of the lane where the subject vehicle is located, and α_{cancel} is the value of α, when the target vehicle in adjacent lane is first detected canceling the lane-changing intention.

During the lane-changing cancellation process of the target vehicle in adjacent lane, $d_{y,\text{adjacentlane}}$ will change from $d_{y,\text{cancel}}$ to 2.875m (When the lateral relative distance of the target in the current lane is greater than 2.875m, this target can be considered as the target in the adjacent lane.), and β will smoothly transfer from α_{cancel} to 0.

5 Longitudinal motion control algorithm

According to whether there is a target vehicle ahead, the longitudinal motion control can be divided into speed control and following control. When there is no target vehicle in front of the subject vehicle, it is divided into speed control. In the speed control, only the subject vehicle speed $v_{subject}$ needs to be kept at the set speed v_{set}. Therefore, the control target in this mode is: $\Delta v \to 0$ and the position error can be directly set to zero:

$$\Delta v = v_{set} - v_{subject} \tag{21}$$

$$\Delta d = 0 \tag{22}$$

When there is a target vehicle in front of the subject vehicle, it is divided into following control, that is, to control the speed of the subject vehicle to keep the same as that of the target vehicle, and meanwhile to keep a safe distance between the subject vehicle and the target vehicle. The constant time-gap safe distance is selected as the safe distance in this paper [27], which is calculated as follows:

$$d_{des} = v_{self}\tau_{\text{h}} + d_0 \tag{23}$$

where τ_h is the time gap constant, generally set to 1.2-2s. d_0 is the distance constant, generally set to 2-3m. In this paper, τ_h is set to 2s, and d_0 is set to 3m.

In the following control, the subject vehicle speed needs to be kept the same as the target vehicle, and the distance d_x between the subject vehicle and the target vehicle needs to be controlled as the safe distance d_{des}, so the control target in this mode is: $\Delta v \to 0, \Delta d \to 0$, where

$$\Delta v = v_x \tag{24}$$

$$\Delta d = d_x - d_{des} \tag{25}$$

LQR controller is chosen to calculate the desired acceleration of the subject vehicle in this paper. The balance state in the longitudinal motion control is $\Delta v \to 0, \Delta d \to 0$, so it is very suitable to use the LQR controller to calculate the desire acceleration of the subject vehicle. At the same time, the LQR controller can consider the weight of the input variable and the state variable to obtain a good ride comfort during the longitudinal motion control.

There is a time delay between the actual acceleration a_{actual} and the input desired acceleration a_{des}, which can be approximately represented by one-order inertia element:

$$a_{actual} = \frac{1}{\tau_d s + 1} a_{des} \tag{26}$$

where τ_d is the time delay between the actual acceleration a_{actual} and the input desired acceleration a_{des}, which is set to 0.5s in this paper.

Select the state variable as $x = [\Delta d, \Delta v, a_{actual}]'$ and the input variable as a_{des}, we can get the continuous state space equation for longitudinal acceleration control:

$$\begin{bmatrix} \dot{\Delta d} \\ \dot{\Delta v} \\ \dot{a}_{actual} \end{bmatrix} = \begin{bmatrix} 0 & 1 & -\tau_h \\ 0 & 0 & -1 \\ 0 & 0 & -1/\tau_d \end{bmatrix} \begin{bmatrix} \Delta d \\ \Delta v \\ a_{actual} \end{bmatrix} + \begin{bmatrix} 0 \\ 0 \\ 1/\tau_d \end{bmatrix} a_{des} + \begin{bmatrix} 0 \\ 1 \\ 0 \end{bmatrix} a_{tar} \tag{27}$$

where a_{tar} is the acceleration of the target vehicle, which is an interference term.

Discretize the above continuous state space equation to obtain:

$$\begin{bmatrix} \Delta d \\ \Delta v \\ a_{actual} \end{bmatrix}_{k+1} = \begin{bmatrix} 1 & T & -\tau_h T \\ 0 & 1 & -T \\ 0 & 0 & 1 - T/\tau_d \end{bmatrix} \begin{bmatrix} \Delta d \\ \Delta v \\ a_{actual} \end{bmatrix}_k + \begin{bmatrix} 0 \\ 0 \\ T/\tau_d \end{bmatrix} a_{des} + \begin{bmatrix} 0 \\ T \\ 0 \end{bmatrix} a_{tar} \tag{28}$$

where T is the control cycle.

Since the ride comfort is greatly affected by the jerk (the derivative of the acceleration), the above-mentioned state space equation cannot take into account the weight of the jerk. Therefore, this paper expands the discrete state space equation to an incremental form, and takes the desired acceleration increment Δa_{des} as input to realize the consideration of the weight of jerk. The expanded state space equation is as follows:

$$\begin{bmatrix} \Delta d \\ \Delta v \\ a_{actual} \\ a_{des} \end{bmatrix}_{k+1} = \begin{bmatrix} 1 & T & -\tau_h T & 0 \\ 0 & 1 & -T & 0 \\ 0 & 0 & 1 - T/\tau_d & T/\tau_d \\ 0 & 0 & 0 & 1 \end{bmatrix} \begin{bmatrix} \Delta d \\ \Delta v \\ a_{actual} \\ a_{des} \end{bmatrix}_k + \begin{bmatrix} 0 \\ 0 \\ T/\tau_d \\ 1 \end{bmatrix} \Delta a_{des} + \begin{bmatrix} 0 \\ T \\ 0 \\ 0 \end{bmatrix} a_{tar} \tag{29}$$

The objective function of the LQR controller is:

$$J = \frac{1}{2} \int_0^\infty \left[q_{l1} \cdot \Delta d^2 + q_{l2} \cdot \Delta v^2 + q_{l3} \cdot a_{actual}^2 + q_{l4} \cdot a_{des}^2 + r_l \cdot u^2 \right] dt \tag{30}$$

where u is the desired acceleration increment Δa_{des} $q_{l1}, q_{l2}, q_{l3}, q_{l4}, r_l$ are represent the weight of $\Delta v, \Delta d, a_{actual}, a_{des}, \Delta a_{des}$ respectively. $q_{l1} = 2$, $q_{l2} = 1$, $q_{l3} = 0$, $q_{l4} = 3$, $r_l = 3$ in this paper.

After the desired acceleration of the subject vehicle is calculated by the LQR controller, it is necessary to control the actuator of the subject vehicle (the throttle opening and the brake master cylinder pressure) to make the actual acceleration of the subject vehicle approach the calculated desired acceleration. This paper first establishes the inverse dynamics model of the subject vehicle. Through the inverse dynamics model, the feedforward control quantity of the actuator can be obtained. Due to the deviation of the subject vehicle's inverse dynamics model parameters and the presence of interference, it is difficult to make the actual acceleration approach the desired acceleration stably by using open-loop control alone. There will be a large static error. Therefore, in order to improve the accuracy and robustness of the longitudinal acceleration control, this paper takes the deviation value between the actual vehicle acceleration and the desired acceleration as input, and uses the PID controller to calculate the feedback control quantity of the actuator.

6 Simulation and discussion

In this section, the co-simulation platform is built based on Matlab/Simulink, CarSim and Prescan software to verify the proposed algorithm. The scenario and sensor models are established in Prescan. The measurement data of the millimeter wave radar model in Prescan contains some noise, which can simulate the radar measurement data in

the real world to a certain extent. The high-precision vehicle dynamics model is established in Carsim, and the simulation environment integration and control algorithm are established in Matlab/Simulink.

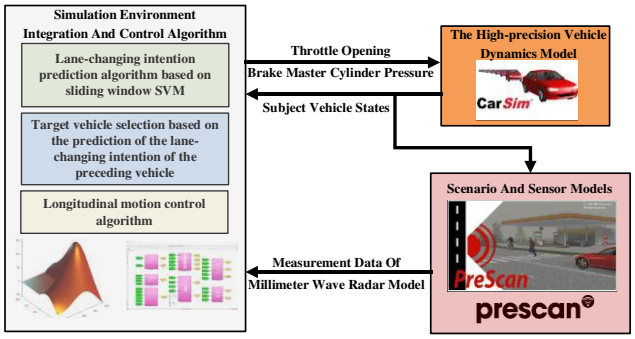

Figure 18 The closed-loop block diagram of Matlab/Simulink, CarSim and Prescan in the co-simulation platform

Simulations are conducted under three different conditions: safe lane-changing condition, dangerous lane-changing condition, and lane-changing cancellation condition.

6.1 Simulation results under safe lane-changing condition

In order to verify the effectiveness of the target vehicle selection algorithm proposed in this paper under safe lane-changing condition, the following simulation conditions are designed in the co-simulation platform: At the initial time, the subject vehicle follows the preceding vehicle in the current lane at the set speed, which is 25m/s, and the longitudinal relative distance between the subject vehicle and the preceding vehicle in the current lane is 50m. In the left adjacent lane, there is a preceding vehicle. The driving speed of the preceding vehicle in the adjacent lane at the start of the simulation is 18m/s, and the longitudinal relative distance to the subject vehicle is 70m. The preceding vehicle starts to change lanes at 5s after the start of the simulation. The simulation results are shown in Figure 19 and Figure 20.

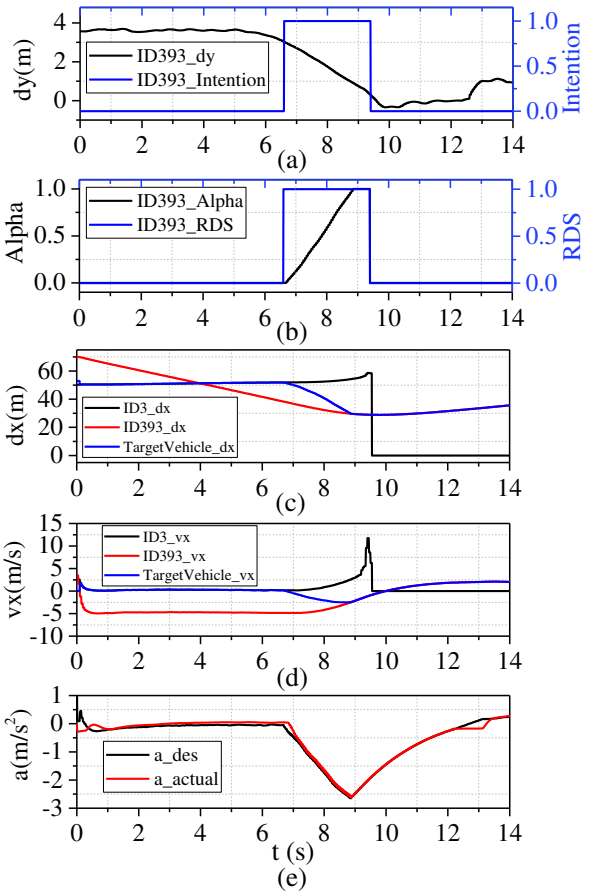

Figure 19 Simulation results of longitudinal control based on lane-changing intention prediction of preceding vehicle under safe lane-changing condition: (a) lateral relative distance and lane-changing intention of the preceding vehicle in the adjacent lane ID393; (b) α and *RDS* of the preceding vehicle in the adjacent lane ID393; (c) relative longitudinal distance of the preceding vehicle in the current lane ID3, the preceding vehicle in the current lane ID393, the target vehicle; (d) relative longitudinal velocity of the preceding vehicle in the current lane ID3, the preceding vehicle in the current lane ID393, the target vehicle; (e) desired longitudinal acceleration and actual longitudinal acceleration of the subject vehicle

At 6.6s after the start of the simulation, the lane-changing intention prediction algorithm based on sliding window SVM detects that the preceding vehicle in the adjacent lane has the lane-changing intention, and the *RDS* is 1, which means the target vehicle in the adjacent lane has the lane-changing intention and there is no risk of collision. Therefore, the target vehicle selection algorithm needs to fuse the target vehicle in the current lane with the target vehicle in the adjacent lane. The result of the fusion is shown in Figure 19(c)(d). The target vehicle smoothly transitions from the target vehicle in the current lane (ID3) to the target vehicle in the adjacent lane (ID393). According to Figure 20(b)(c), when using the target

vehicle selection method of the traditional ACC system, the target vehicle jumps directly from the target vehicle in the current lane to the target vehicle in the adjacent lane at the 7.8s. The lane-changing intention prediction algorithm based on sliding window SVM designed in this paper can identify the lane-changing intention of the preceding vehicle 1.2s in advance, compared with the target vehicle selection method of the traditional ACC system. In addition, the state of the target vehicle in the current lane changes suddenly at 9.4s in Figure 19(c)(d). That is because the target vehicle in the current lane will be blocked and cannot be detected by the sensor of the subject vehicle when the lane change of the target vehicle in the adjacent lane is completed.

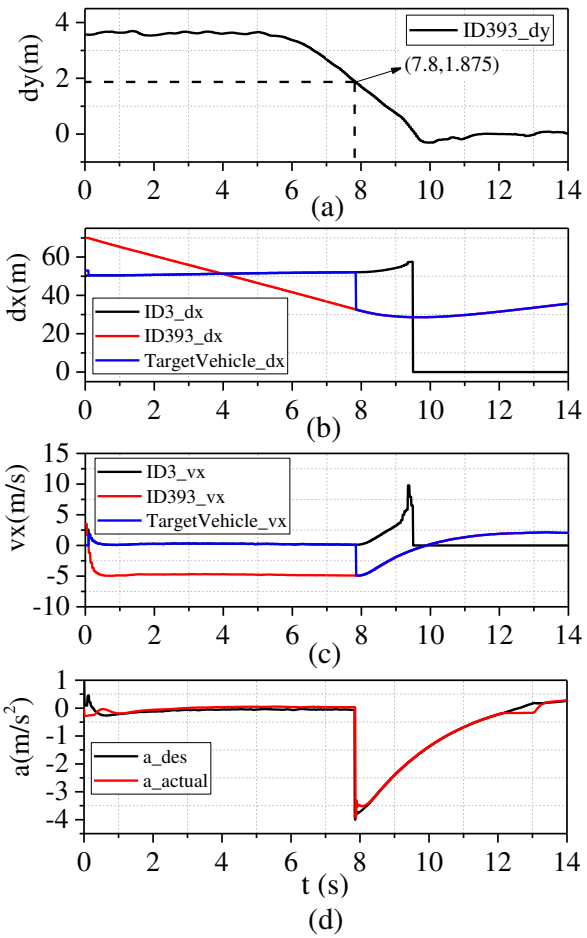

Figure 20 Simulation results of traditional ACC longitudinal control under safe lane-changing condition: (a) lateral relative distance of the preceding vehicle in the adjacent lane ID393; (b) relative longitudinal distance of the preceding vehicle in the current lane ID3, the preceding vehicle in the current lane ID393, the target vehicle; (c) relative longitudinal velocity of the preceding vehicle in the current lane ID3, the preceding vehicle in the current lane ID393, the target vehicle; (d) desired longitudinal acceleration and actual longitudinal acceleration of the subject vehicle

Figure 19(e) and Figure 20(d) show the longitudinal acceleration curve of the subject vehicle under safe lane-changing condition. It can be seen from the simulation results that the maximum longitudinal deceleration of the subject vehicle is 2.62m/s^2 during the entire control process by using the target vehicle algorithm proposed in this paper. When using the target vehicle selection method of the traditional ACC system, the maximum longitudinal deceleration of the subject vehicle is 3.90m/s^2. The target vehicle selection algorithm proposed in this paper can make a faster response to the lane change of the preceding vehicle in the adjacent lane, 1.25s ahead of time. And the corresponding maximum longitudinal deceleration is reduced by 1.28m/s^2. It can effectively reduce the fluctuation of the longitudinal acceleration of the subject vehicle and improve the riding comfort, caused by the safe lane change of the preceding vehicle in the adjacent lane.

6.2 Simulation results under dangerous lane-changing condition

At the initial time, the subject vehicle follows the preceding vehicle in the current lane at the set speed, the driving speed is 25m/s, and the longitudinal relative distance between the subject vehicle and the preceding vehicle in the current lane is 50m. The driving speed of the preceding vehicle in the adjacent lane at the start of the simulation is 15m/s, and the longitudinal relative distance to the subject vehicle is 70m. The preceding vehicle starts to change lanes at 4.5s after the start of the simulation. The simulation results are shown in Figure 21 and Figure 22.

At 5.5s after the start of the simulation, the lane-changing intention prediction algorithm based on sliding window SVM detects that the preceding vehicle in the adjacent lane has the lane-changing intention, and the *RDS* is 2, which means the target vehicle in the adjacent lane has the lane-changing intention and there is a risk of collision. In this case, priority should be given to the target vehicle in the adjacent lane. The result is shown in Figure 21(c)(d). The target vehicle selection algorithm proposed in this paper jumps directly from the target vehicle in the current lane to the target vehicle in the adjacent lane when the lane-changing intention is detected. According to Figure 22(b)(c), when using the target vehicle selection method of the traditional ACC algorithm, the target vehicle jumps directly from the target vehicle in the current lane to the target vehicle in the adjacent lane at the 6.25s when the target vehicle in the adjacent lane crosses the lane line. The lane-changing intention prediction algorithm based on sliding window SVM designed in this paper can identify the lane-changing intention of the preceding vehicle 0.75s in advance, compared with the traditional ACC target vehicle selection algorithm.

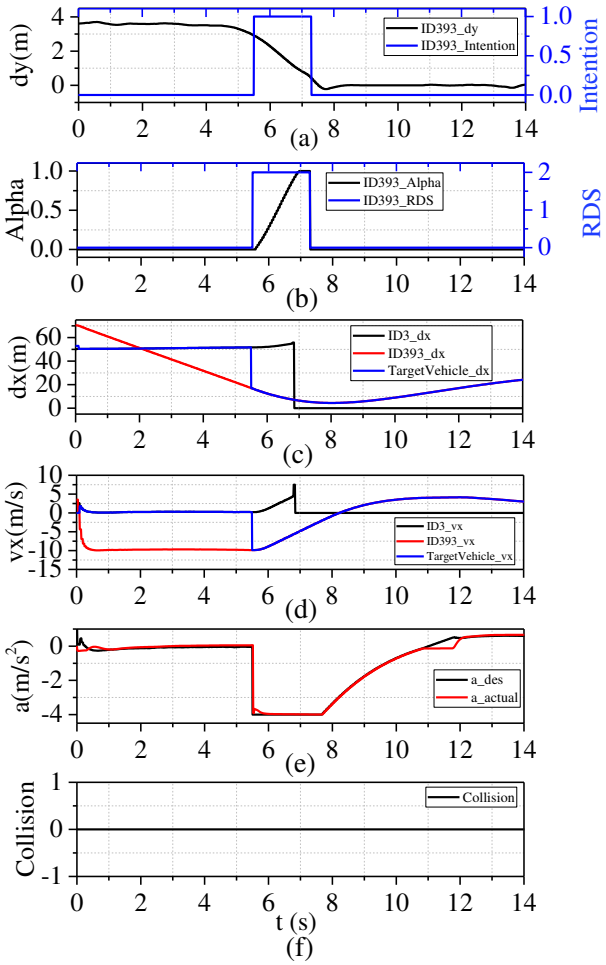

Figure 21 Simulation results of longitudinal control based on lane-changing intention prediction of preceding vehicle under dangerous lane-changing condition: (a) lateral relative distance and lane-changing intention of the preceding vehicle in the adjacent lane ID393; (b) α and *RDS* of the preceding vehicle in the adjacent lane ID393; (c) relative longitudinal distance of the preceding vehicle in the current lane ID3, the preceding vehicle in the current lane ID393, the target vehicle; (d) relative longitudinal velocity of the preceding vehicle in the current lane ID3, the preceding vehicle in the current lane ID393, the target vehicle, (e) desired longitudinal acceleration and actual longitudinal acceleration of the subject vehicle; (f) collision during longitudinal control

Figure 21(e) and Figure 22(d) show the longitudinal acceleration curve of the subject vehicle under dangerous lane-changing condition. Figure 21(f) and Figure 22(e) show the collision signal between the subject vehicle and the surrounding traffic vehicles. It can be seen from the simulation results that the maximum longitudinal deceleration of the subject vehicle by using the target vehicle selection algorithm proposed in this paper and the target vehicle selection method of the traditional ACC system both reach the maximum value 4m/s2. However, the target vehicle selection algorithm proposed in this paper can make a faster response to the lane change of the preceding vehicle in the adjacent lane, 0.75s ahead of time. From Figure 21(f) and Figure 22(e), the subject vehicle collides with the target vehicle in the adjacent lane at 7.56s when using the target vehicle selection method of the traditional ACC system. Because of the target vehicle selection method proposed in this paper, the subject vehicle can decelerate 0.75s in advance, and the minimum longitudinal relative distance between the subject vehicle and the target vehicle in the adjacent lane is 4.5m, effectively avoiding collision.

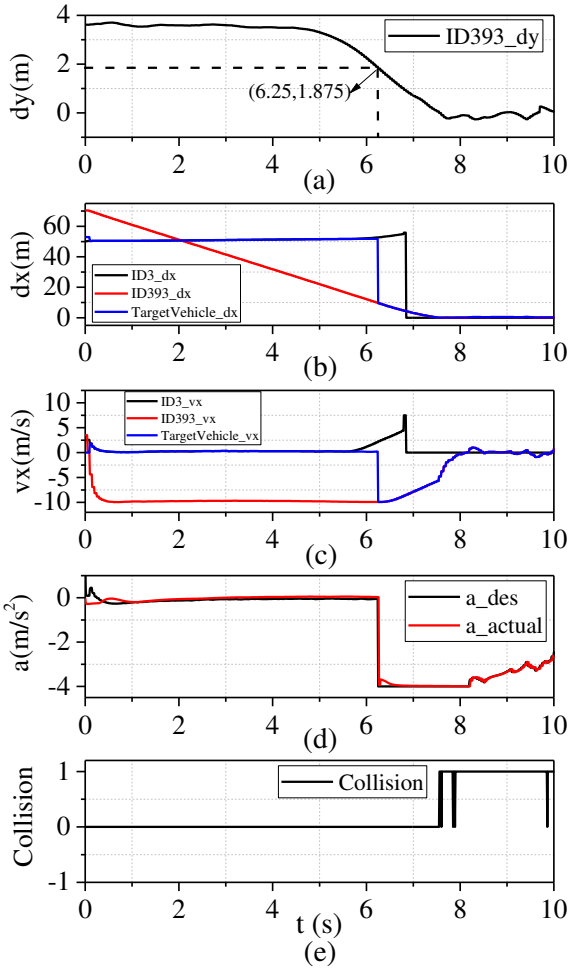

Figure 22 Simulation results of traditional ACC longitudinal control under dangerous lane-changing condition: (a) lateral relative distance of the preceding vehicle in the adjacent lane ID393; (b) relative longitudinal distance of the preceding vehicle in the current lane ID3, the preceding vehicle in the current lane ID393, the target vehicle; (c) relative longitudinal velocity of the preceding vehicle in the current lane ID3, the preceding vehicle in the current lane ID393, the target vehicle; (d) desired longitudinal acceleration and actual longitudinal acceleration of the subject vehicle; (e) collision during longitudinal control

6.3 Simulation results under lane-changing cancellation condition

At the initial time, the subject vehicle follows the preceding vehicle in the current lane at the set speed, the driving speed is 25m/s, and the longitudinal relative distance between the subject vehicle and the preceding vehicle in the current lane is 50m. The driving speed of the preceding vehicle in the adjacent lane at the start of the simulation is 20m/s, and the longitudinal relative distance to the subject vehicle is 70m. The preceding vehicle starts to change lanes at 4.5s after the start of the simulation. The simulation results are shown in Figure 23 and Figure 24.

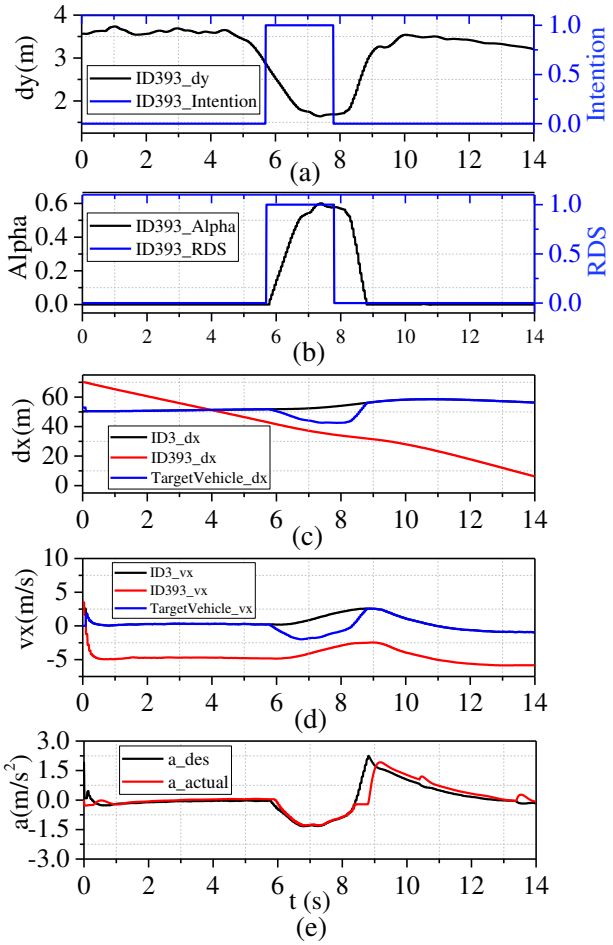

Figure 23 Simulation results of longitudinal control based on lane-changing intention prediction of preceding vehicle under lane-changing cancellation condition: (a) lateral relative distance and lane-changing intention of the preceding vehicle in the adjacent lane ID393; (b) α and *RDS* of the preceding vehicle in the adjacent lane ID393; (c) relative longitudinal distance of the preceding vehicle in the current lane ID3, the preceding vehicle in the current lane ID393, the target vehicle; (d) relative longitudinal velocity of the preceding vehicle in the current lane ID3, the preceding vehicle in the current lane ID393, the target vehicle; (e) desired longitudinal acceleration and actual longitudinal acceleration of the subject vehicle

At 5.7s after the start of the simulation, the lane-changing intention prediction algorithm based on sliding window SVM detects that the preceding vehicle in the adjacent lane has the lane-changing intention, and the *RDS* is 1, which means the target vehicle in the adjacent lane has the lane-changing intention and there is no risk of collision. Therefore, the target vehicle selection algorithm needs to fuse the target vehicle in the current lane with the target vehicle in the adjacent lane. The result of the fusion is shown in Figure 23(c)(d) above. The target vehicle smoothly transitions from the target vehicle in the current lane (ID3) to the target vehicle in the adjacent lane (ID393).

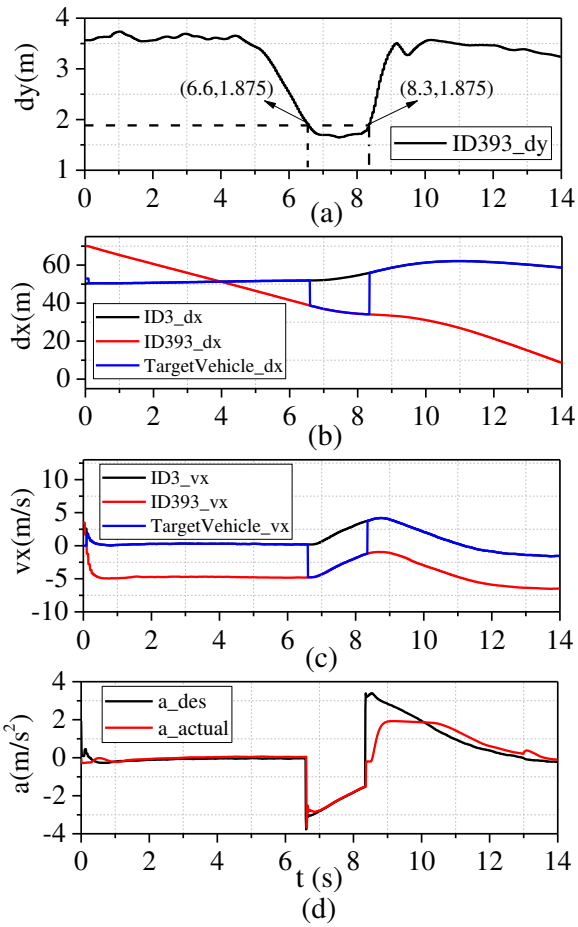

Figure 24 Simulation results of traditional ACC longitudinal control under lane-changing cancellation condition: (a) lateral relative distance of the preceding vehicle in the adjacent lane ID393; (b) relative longitudinal distance of the preceding vehicle in the current lane ID3, the preceding vehicle in the current lane ID393, the target vehicle; (c) relative longitudinal velocity of the preceding vehicle in the current lane ID3, the preceding vehicle in the current lane ID393, the target vehicle; (d) desired

longitudinal acceleration and actual longitudinal acceleration of the subject vehicle

Before lane change is completed, lane-changing intention prediction algorithm based on sliding window SVM detects that the target vehicle in the adjacent lane cancels lane change at 7.8s, and the α is 0.58 at this time. If the target vehicle directly changes back to the target vehicle in the current lane, it will inevitably lead to the jump of the target vehicle. Therefore, it is necessary to select the target vehicle according to the target vehicle selection algorithm under lane-changing cancellation condition, so that the target vehicle can smoothly transition back to the target vehicle in the current lane. The target vehicle information is shown in Figures 23(c)(d), and the variation curve of α is shown in the Figures 23(b).

When using the target vehicle selection method of the traditional ACC system, the target vehicle jumps directly from the target vehicle in current lane to the target vehicle in the adjacent lane because the target vehicle in the adjacent lane crosses the left lane line at the 6.6s. And at 8.3s, since the target vehicle in the adjacent lane crosses the left lane line and returned to its original lane, the target vehicle changes from the target vehicle in the adjacent lane back to the target vehicle in current lane. Figure 23(e) and Figure 24(d) show the longitudinal acceleration of the subject vehicle under lane-changing cancellation condition. It can be seen from the simulation results that the maximum longitudinal deceleration of the subject vehicle is 1.94m/s^2 during the entire control process by using the target vehicle selection algorithm proposed in this paper. When using the target vehicle selection method of the traditional ACC system, the maximum longitudinal deceleration of the subject vehicle is 3.70m/s^2. The maximum longitudinal deceleration is reduced by 1.28m/s^2. However, the maximum acceleration is almost the same. This is because at the current speed, the acceleration of the subject vehicle is limited, which means, within the range of 8.5-10s after the start of the simulation, the throttle opening of the subject vehicle has reached 100%. But from the desired acceleration curve, it can also be seen that through the smooth transition of the target vehicle, the maximum desired acceleration is reduced by about 1.14m/s^2 by using the target vehicle selection algorithm proposed in this paper (the maximum desired acceleration is 2.24m/s^2), compared with the target vehicle selection method of the traditional ACC system (the maximum desired acceleration is 3.38m/s^2).

7 Conclusions

In this paper, a target vehicle selection algorithm based on the prediction of the lane-changing intention of the preceding vehicle is proposed. And the lane-changing intention of the preceding vehicle is identified by the lane-changing intention prediction algorithm based on sliding window SVM, trained by the NGSIM dataset. The lane-changing intention prediction algorithm proposed in this paper is applicable to the preceding vehicle both in the current lane and in the adjacent lane. Through comparison with the target vehicle selection method of the traditional ACC system, the simulation results show that the target vehicle selection algorithm proposed in this paper can respond to the lane change of the preceding vehicle in advance, thus effectively reducing the longitudinal acceleration fluctuation and avoiding the collision under the dangerous lane-changing condition.

As future work, the trajectory of the preceding vehicle will be predicted to further improve the driving safety of the subject vehicle. At the same time, the proposed algorithm will be verified on the real vehicle platform to verify the real-time of the algorithm and its robustness to interference in the real road environment.

8 Declaration

Acknowledgements

The authors sincerely thanks to associate Professor Guo-Ying Chen of Jilin University for his critical discussion and reading during manuscript preparation.

Funding

Supported by National Natural Science Foundation of China (Grant Nos. 51775236 U1564214), and National Key Research and Development Program (Grant No. 2017YFB0102600)

Availability of data and materials

The datasets supporting the conclusions of this article are included within the article.

Authors' contributions

The author' contributions are as follows: Jun Yao and Guo-Ying Chen were in charge of the whole trial; Jun Yao wrote the manuscript; Zhen-Hai Gao reviewed the manuscript. All authors read and approved the final manuscript.

Competing interests

The authors declare no competing financial interests.

Consent for publication

Not applicable

Ethics approval and consent to participate

Not applicable

References

[1] Shah, Puneet. (2019). Adaptive Cruise Control (ACC) Market to Display Significant Growth During Forecast Period. 10.13140/RG.2.2.27676.44163.

[2] Ziegler J , Bender P , Schreiber M , et al. Making Bertha Drive—An Autonomous Journey on a Historic Route[J]. IEEE Intelligent Transportation Systems Magazine, 2014, 6(2):8-20.

[3] Kim J , Kim J , Jang G J , et al. Fast learning method for convolutional neural networks using extreme learning machine and its application to lane detection[J]. Neural Netw, 2017, 87:109-121.

[4] Umberto M , Shilp D , Saber F , et al. Towards connected autonomous driving: review of use-cases[J]. Vehicle System Dynamics, 2018:1-36.

[5] Chen X W , Zhang J G , Liu Y J . Research on the Intelligent Control and Simulation of Automobile Cruise System Based on Fuzzy System[J]. Mathematical Problems in Engineering,2016,(2016-6-29), 2016, 2016(pt.6):1-12.

[6] Martinez J J , Canudas-De-Wit C . A Safe Longitudinal Control for Adaptive Cruise Control and Stop-and-Go Scenarios[J]. IEEE Transactions on Control Systems Technology, 2007, 15:246-258.

[7] Moon S, Kang H, Yi K Multi-vehicle target selection for adaptive cruise control[J], Vehicle System Dynamics: International Journal of Vehicle Mechanics and Mobility, 2010, 48:11, 1325-1343.

[8] Kim D , Moon S , Kim H J , et al. Design of an Adaptive Cruise Control / Collision Avoidance with lane change support for vehicle autonomous driving[C]// Iccas-sice. IEEE, 2009.

[9] Ma G, Liu Z, Pei X, et al. Identification of Cut-in Maneuver of Side Lane Vehicles Based on Fuzzy Support Vector Machines[J]. Automotive Engineering, 2014, 36(3):316-320. (in Chinese)

[10] Zou Y, Wei S, Ma G, et al. A Research on the Side-lane Vehicle Cut-in Control in Adaptive Cruise Control System[J]. Automotive Engineering, 2016, 38(03):323-329. (in Chinese)

[11] Woo H, Ji Y, Kono, H, et al. Lane-Change Detection Based on Vehicle-Trajectory Prediction[J]. IEEE Robotics and Automation Letters, 2017, PP. 1-1. 10.1109/LRA.2017.2660543.

[12] Ma S. RESEARCH ON INTELLIGENT VEHICLE LANE CHANGING BEHAVIOR JUDGMENT AND COLLISION RISK ESTIMATION[D]. Harbin Institute of Technology, 2016. (in Chinese)

[13] Zhang K. RECOGNITION METOOD OF LANE-CHANGING BEHAVIOUR AND DANGER LEVEL FOR INTELLIGENT VEHICLE[D]. Harbin Institute of Technology, 2017. (in Chinese)

[14] Mitrovic D. Reliable Method for Driving Events Recognition[J]. IEEE Transactions on Intelligent Transportation Systems, 2005, 6(2):p.198-205.

[15] ZHANG H, Fu R. Driving Behavior Recognition and Intention Prediction of Adjacent Preceding Vehicle in Highway Scene[J]. Journal of Transportation Systems Engineering and Information Technology, 2020,20(01): 40-46. (in Chinese)

[16] Yoon S , Jeon H , Kum D . Predictive Cruise Control Using Radial Basis Function Network-Based Vehicle Motion Prediction and Chance Constrained Model Predictive Control[J]. IEEE Transactions on Intelligent Transportation Systems, 2019, PP(99):1-12.

[17] Lee D , Kwon Y P , Mcmains S , et al. Convolution Neural Network-based Lane Change Intention Prediction of Surrounding Vehicles for ACC[C]// IEEE 20th International Conference on Intelligent Transportation Systems. IEEE, 2017.

[18] FHWA, U.S. Department of Transportation. NGSIM–Next Generation Simulation. (2020-3-11). http://ops.fhwa.dot.gov/trafficanalysistools/ngsim.htm. Accessed July 30, 2012.

[19] P. Kumar, M. Perrollaz, S. Lefevre, and C. Laugier, Learning based approach for online lane change intention prediction, Proceedings of the IEEE International Conference on Intelligent Vehicle Symposium, 2013, pp. 797-802.

[20] K. P. Bennett and E. J. Bredensteiner, Duality and geometry in SVM classifiers, in Proceedings of the 17th International Conference on Machine Learning, 2000, pp. 57-64.

[21] Amsalu S B , Homaifar A , Afghah F , et al. Driver behavior modeling near intersections using support vector machines based on statistical feature extraction[C]// Intelligent Vehicles Symposium. IEEE, 2015.

[22] Werling M , Ziegler J , Kammel S , et al. Optimal Trajectory Generation for Dynamic Street Scenarios in a Frenet Frame[C]. Robotics and Automation (ICRA), 2010 IEEE International Conference on. IEEE, 2010.

[23] Do Carmo M P . Differential Geometry of Curves and Surfaces[M]. Prentice-Hall, 1976.

[24] Vapnik V N . The Nature of Statistical Learning Theory[M]. Springer, 1995.

[25] P. Fancher, Z. Bareket, R. Ervin. Human-Centered Design of an Acc-With-Braking and Forward-Crash-Warning System. 2001, 36(2-3):203-223.

[26] Manjiang H , Yuan L , Wenjun W , et al. Decision Tree-Based Maneuver Prediction for Driver Rear-End Risk-Avoidance Behaviors in Cut-In Scenarios[J]. Journal of advanced transportation, 2017, 2017(7170358).

[27] Wang J , Rajamani R . Should adaptive cruise-control systems be designed to maintain a constant time gap between vehicles?[J]. IEEE Transactions on Vehicular Technology, 2004, 53(5):1480-1490

Biographical notes

Jun Yao, born in 1995, is currently a PhD student at *College of Automotive Engineering, Jilin University, Changchun, China*. He received his bachelor degree from *Jilin University, China*, in July 2020. His research interests include vehicle dynamics and control, and autonomous vehicles.
E-mail: yaojun1995@139.com

Guo-Ying Chen, born in 1984, is currently an associate professor at *Jilin University, China*. He received his PhD degree from *Jilin University, China*, in 2012. His research interests include control-by-wire vehicle control and autonomous vehicles.
E-mail: cgy-011@163.com

Zhen-Hai Gao, is a professor at in *Jilin University, China*. Dr. Gao received his Ph.D. degree in automotive engineering from *Jilin University*, 2000. He was a foreign researcher of the *University of Tokyo*. In recent years, his research has been focused on connected & automated vehicles, driver behavior

analysis, advanced driver assistance system, and human-machine interface.
E-mail: gaozh@jlu.edu.cn

Figures

Figure 1

Schematic diagram of lane change of the preceding vehicle in adjacent lane

Figure 2

Schematic diagram of lane change of the preceding vehicle in adjacent lane

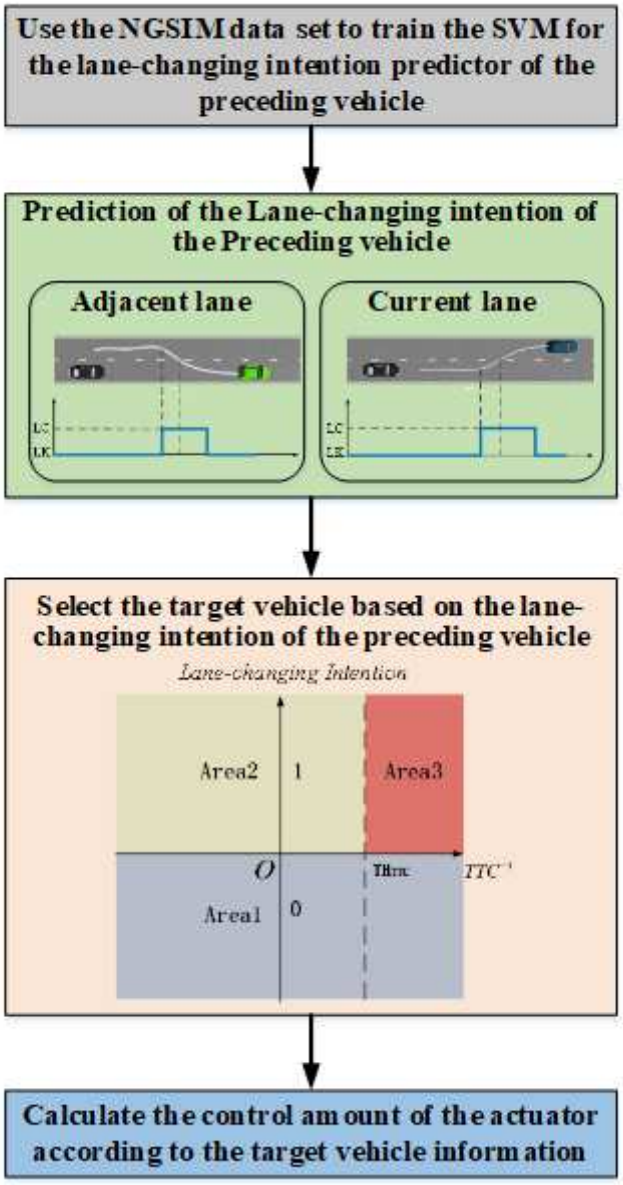

Figure 3

The overall framework of longitudinal control algorithm based on prediction of the lane-changing intention of the preceding vehicle

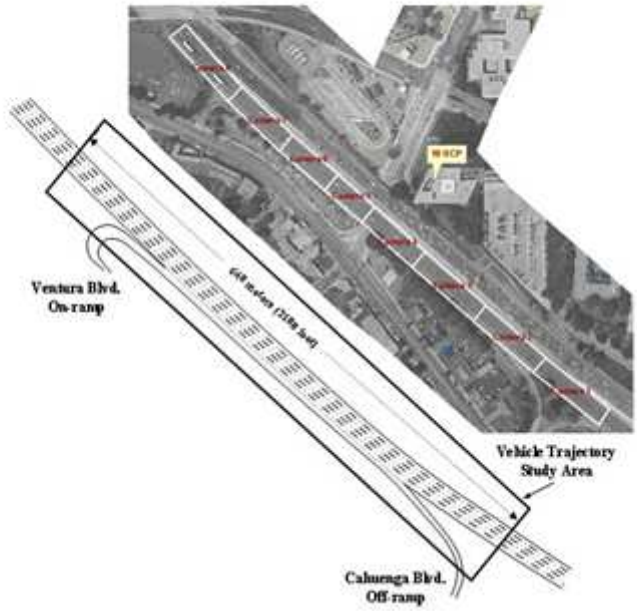

Figure 4

Study area schematic and camera coverage of NGSIM US 101 highway data

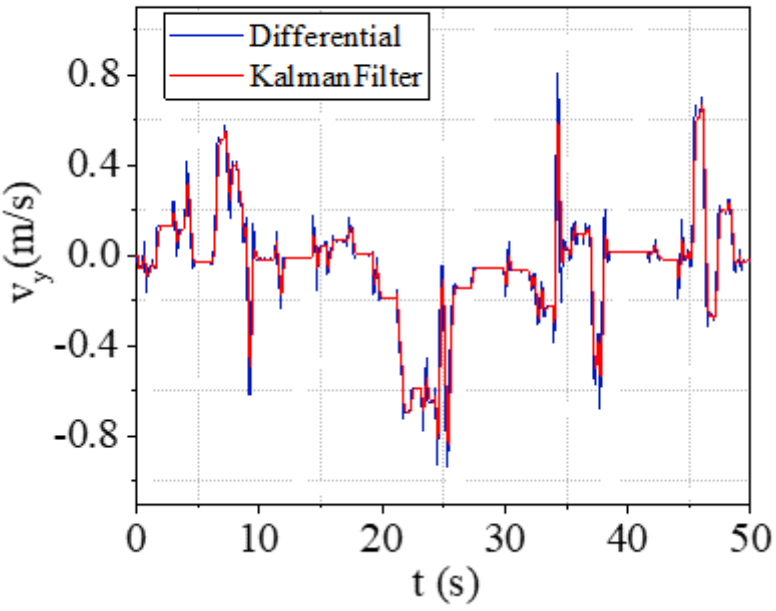

Figure 5

Kalman filtering result of relative lateral velocity

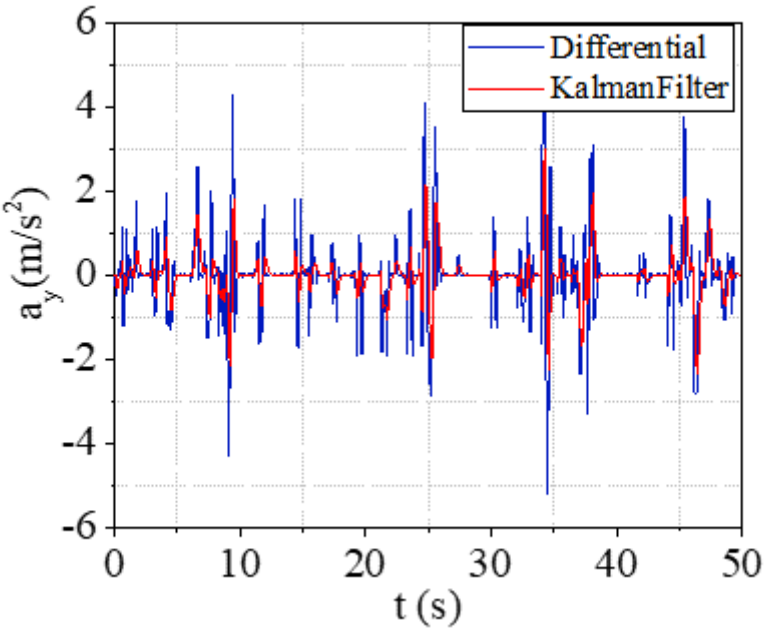

Figure 6

Kalman filtering result of relative lateral acceleration

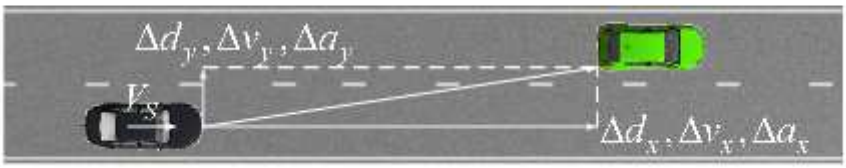

Figure 7

Schematic diagram of feature vector selected in [10]

Figure 8

Schematic diagram of feature vector selected in this paper

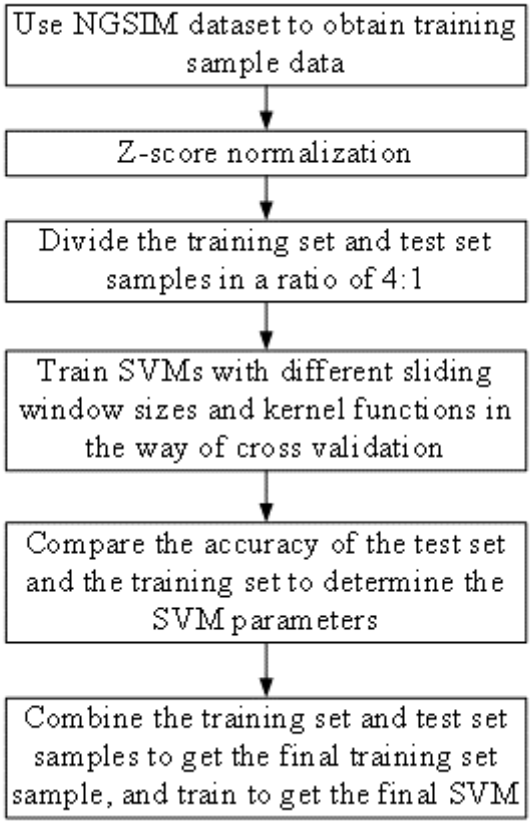

Figure 9

The flow chart of the SVM parameter training

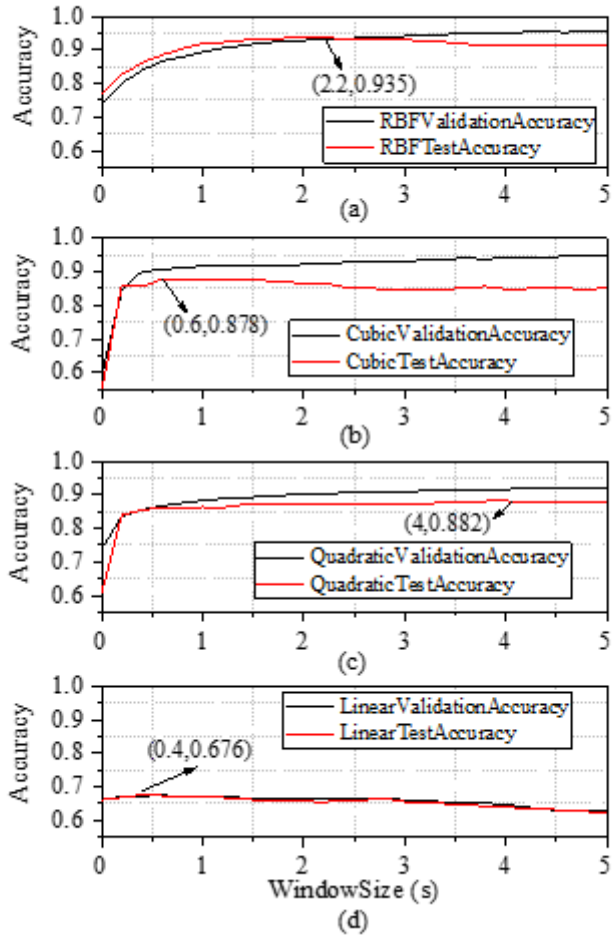

Figure 10

Validation accuracy and test accuracy of SVM with four different kernel functions in the sliding window size range of 0s~5s with an interval of 0.2s

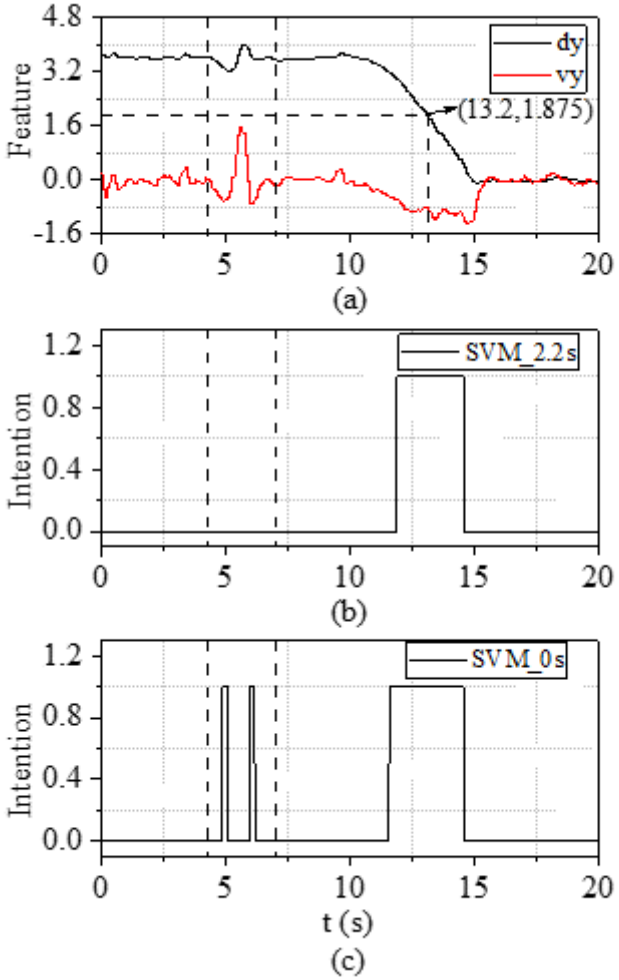

Figure 11

The prediction results of the lane-changing intention of the preceding vehicle in the adjacent lane: (a) features of SVM; (b) the lane-changing intention prediction by SVM_2.2s; (c) the lane-changing intention prediction by SVM_0s

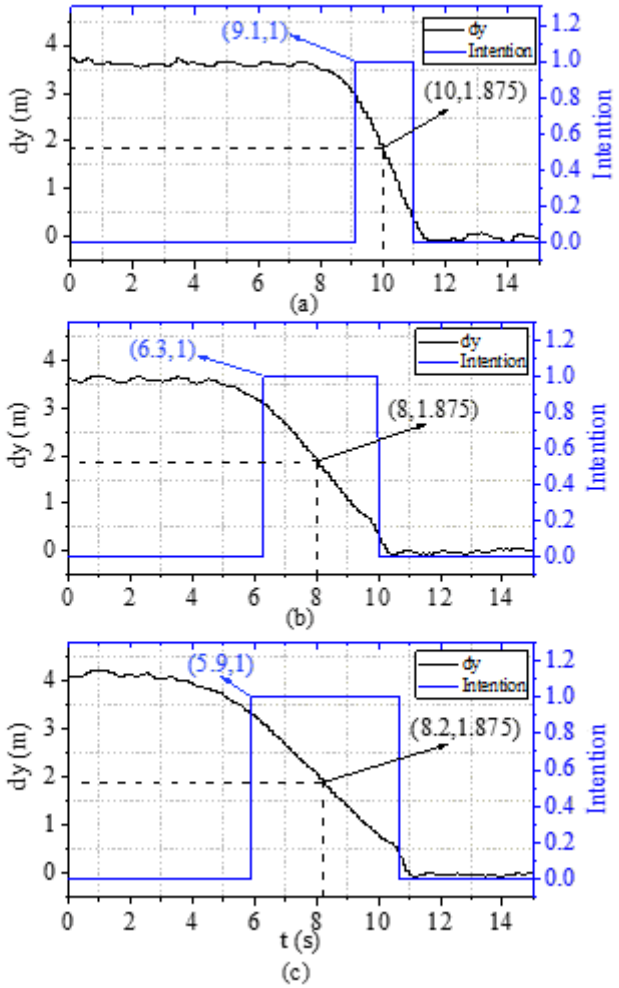

Figure 12

The prediction results of lane-changing intention of the preceding vehicle under three different overall lane-changing times: (a) the overall lane-changing time is 3.1s; (b) the overall lane-changing time is 5.0s; (c) the overall lane-changing time is 6.9s

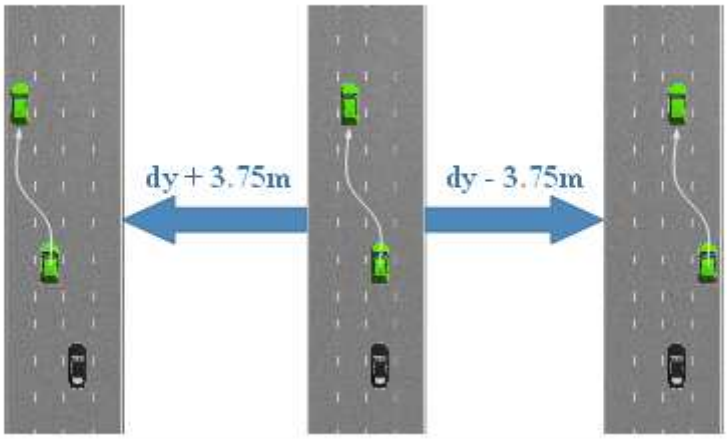

Figure 13

Schematic diagram of relative lateral distance offset

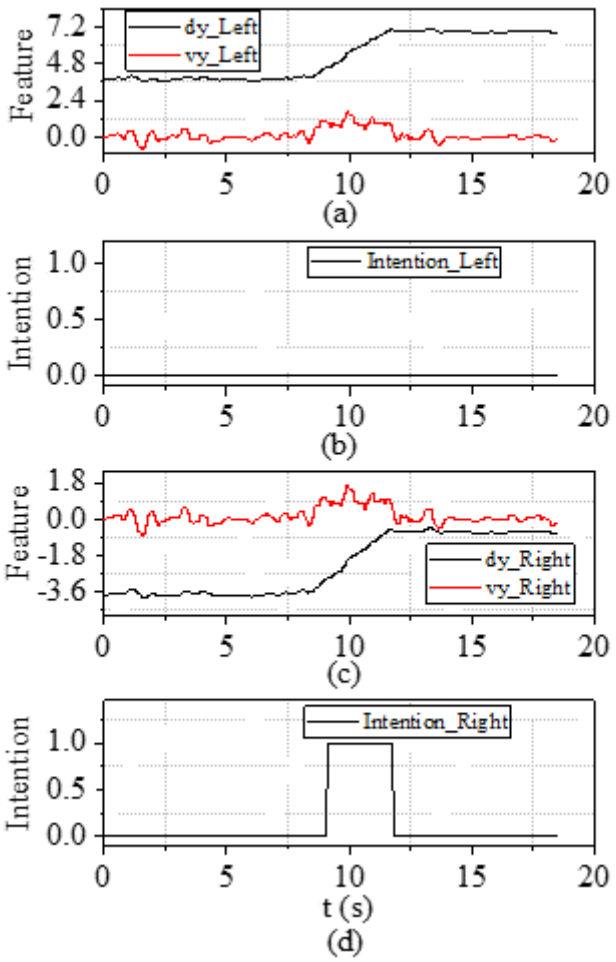

Figure 14

The prediction results of the lane-changing intention of the preceding vehicle in the current lane: (a) features of the left lane-changing intention prediction SVM; (b) the left lane-changing intention prediction; (c) features of the right lane-changing intention prediction SVM; (d) the right lane-changing intention prediction

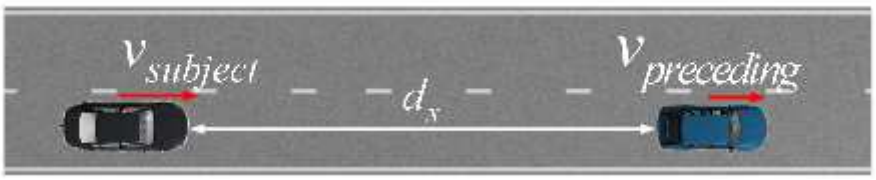

Figure 15

Schematic diagram of the longitudinal relative distance and the longitudinal relative speed

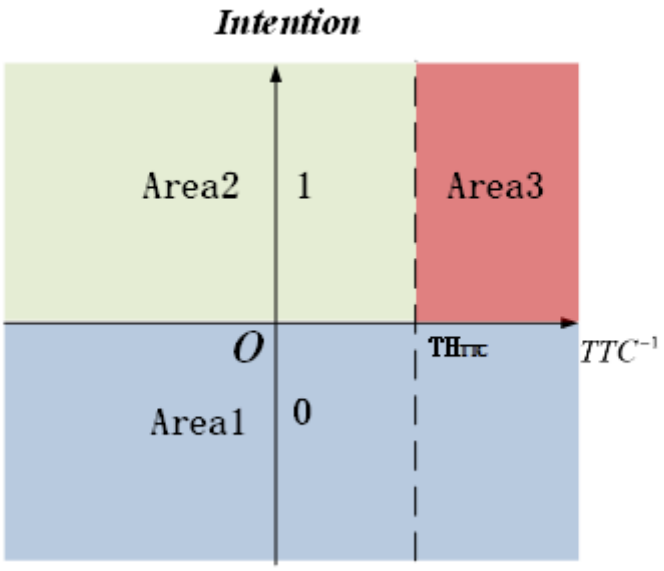

Figure 16

Schematic diagram of DriveStatue of effective target

Figure 17

Schematic diagram of the preceding vehicle's lane-changing cancellation

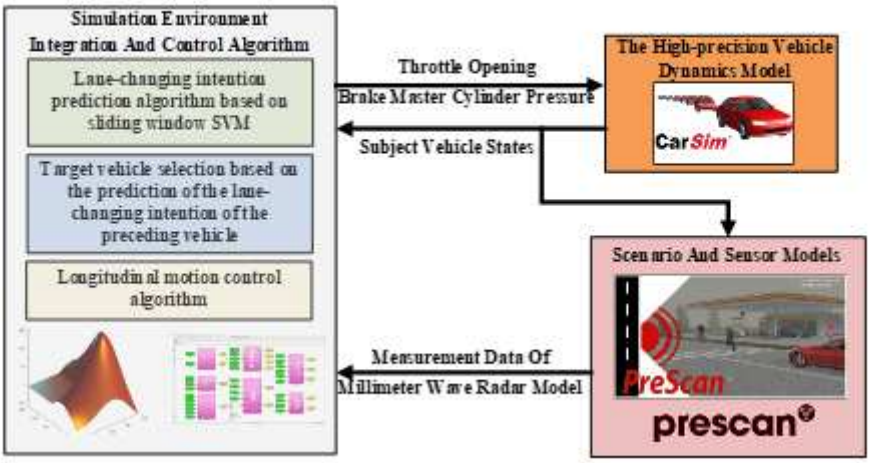

Figure 18

The closed-loop block diagram of Matlab/Simulink, CarSim and Prescan in the co-simulation platform

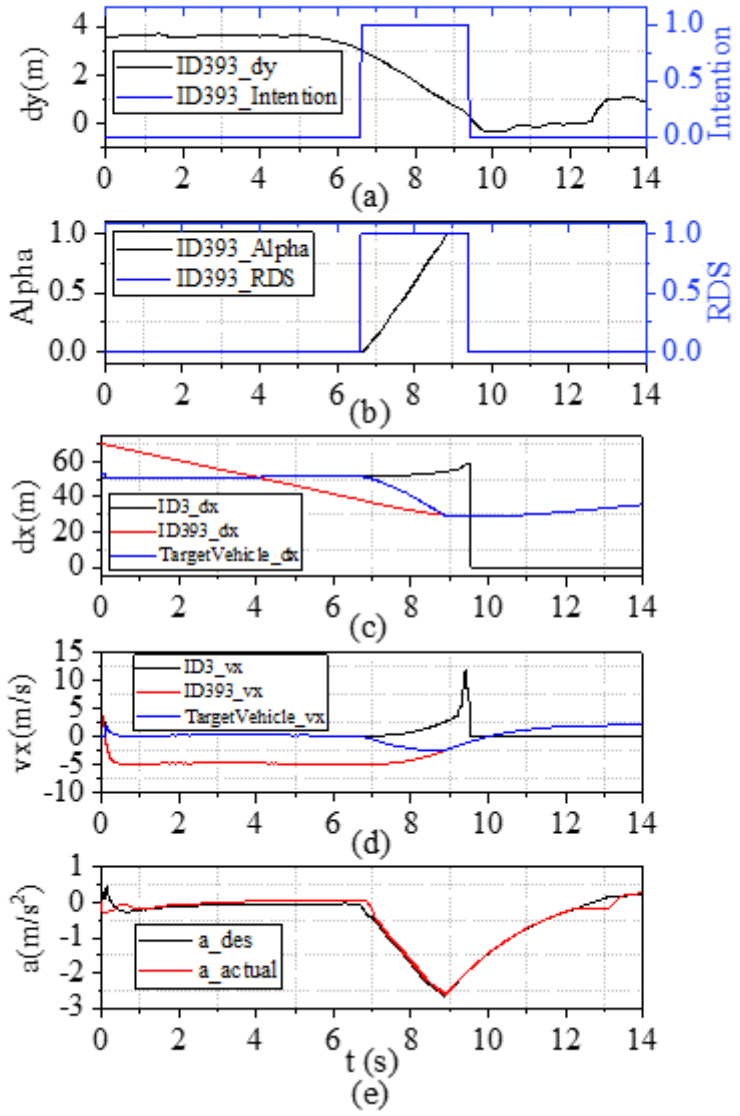

Figure 19

Simulation results of longitudinal control based on lane-changing intention prediction of preceding vehicle under safe lane-changing condition: (a) lateral relative distance and lane-changing intention of the preceding vehicle in the adjacent lane ID393; (b) α and RDS of the preceding vehicle in the adjacent lane ID393; (c) relative longitudinal distance of the preceding vehicle in the current lane ID3, the preceding vehicle in the current lane ID393, the target vehicle; (d) relative longitudinal velocity of the preceding vehicle in the current lane ID3, the preceding vehicle in the current lane ID393, the target vehicle; (e) desired longitudinal acceleration and actual longitudinal acceleration of the subject vehicle

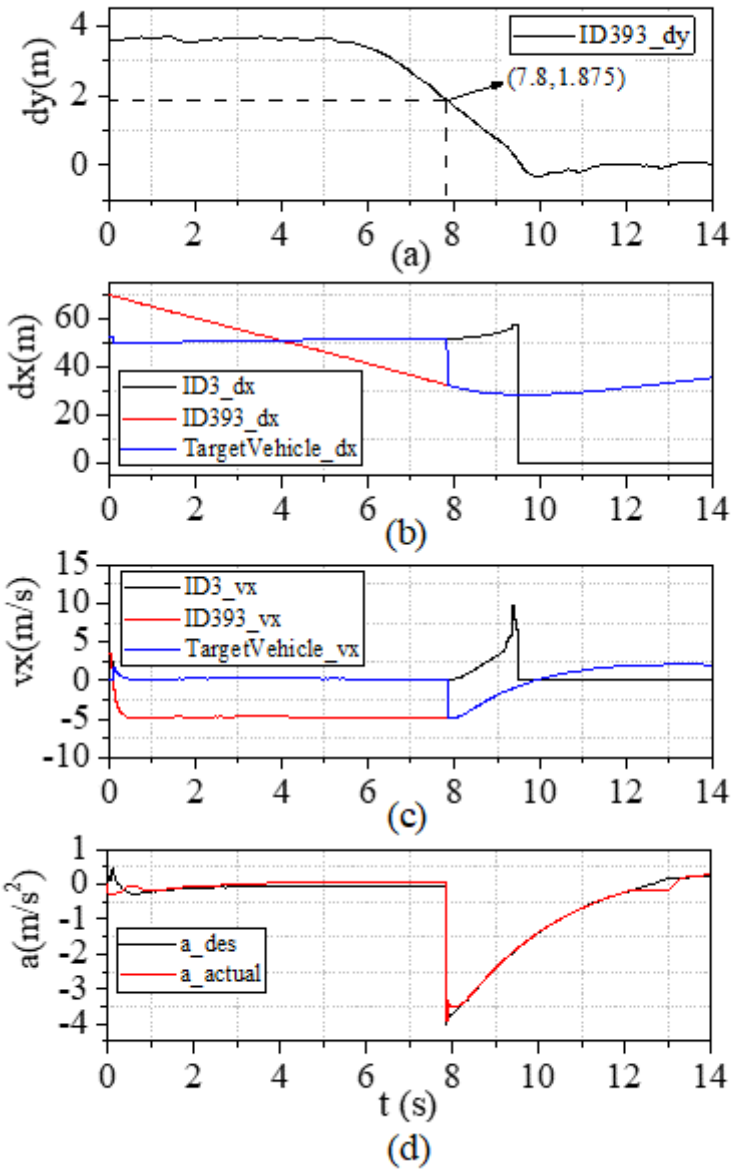

Figure 20

Simulation results of traditional ACC longitudinal control under safe lane-changing condition: (a) lateral relative distance of the preceding vehicle in the adjacent lane ID393; (b) relative longitudinal distance of the preceding vehicle in the current lane ID3, the preceding vehicle in the current lane ID393, the target vehicle; (c) relative longitudinal velocity of the preceding vehicle in the current lane ID3, the preceding vehicle in the current lane ID393, the target vehicle; (d) desired longitudinal acceleration and actual longitudinal acceleration of the subject vehicle

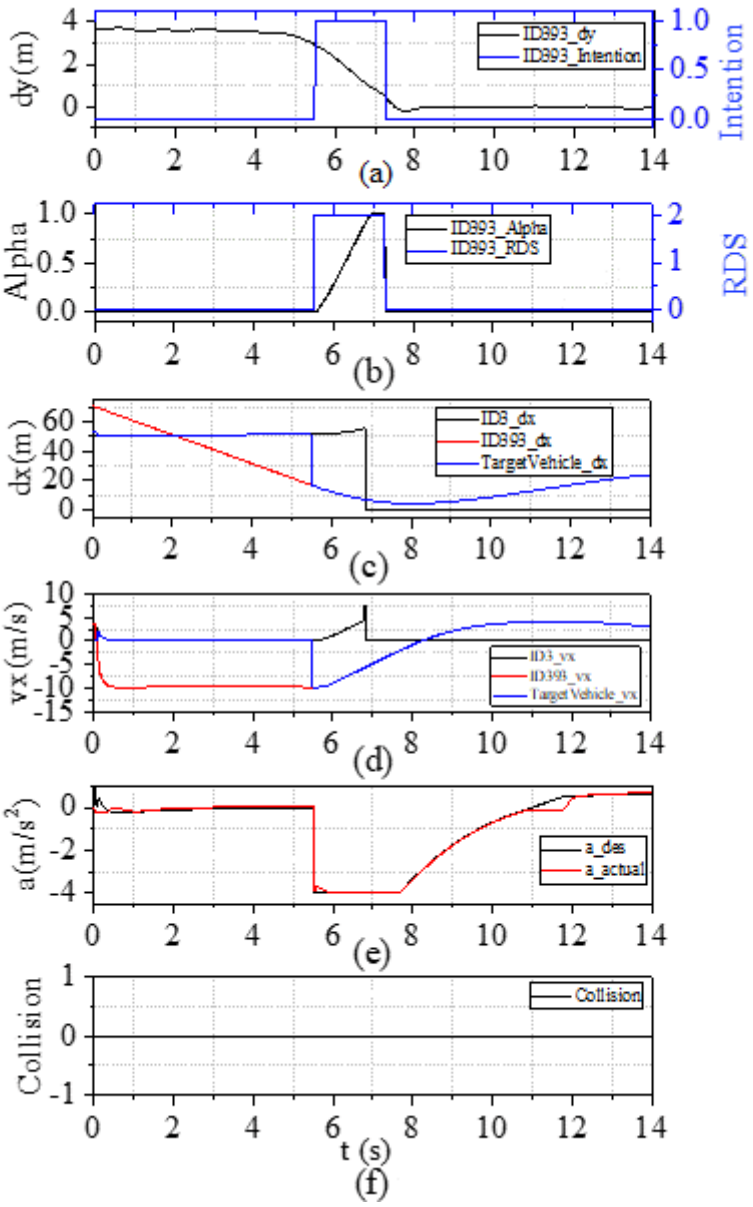

Figure 21

Simulation results of longitudinal control based on lane-changing intention prediction of preceding vehicle under dangerous lane-changing condition: (a) lateral relative distance and lane-changing intention of the preceding vehicle in the adjacent lane ID393; (b) α and RDS of the preceding vehicle in the adjacent lane ID393; (c) relative longitudinal distance of the preceding vehicle in the current lane ID3, the preceding vehicle in the current lane ID393, the target vehicle; (d) relative longitudinal velocity of the preceding vehicle in the current lane ID3, the preceding vehicle in the current lane ID393, the target vehicle, (e) desired longitudinal acceleration and actual longitudinal acceleration of the subject vehicle; (f) collision during longitudinal control

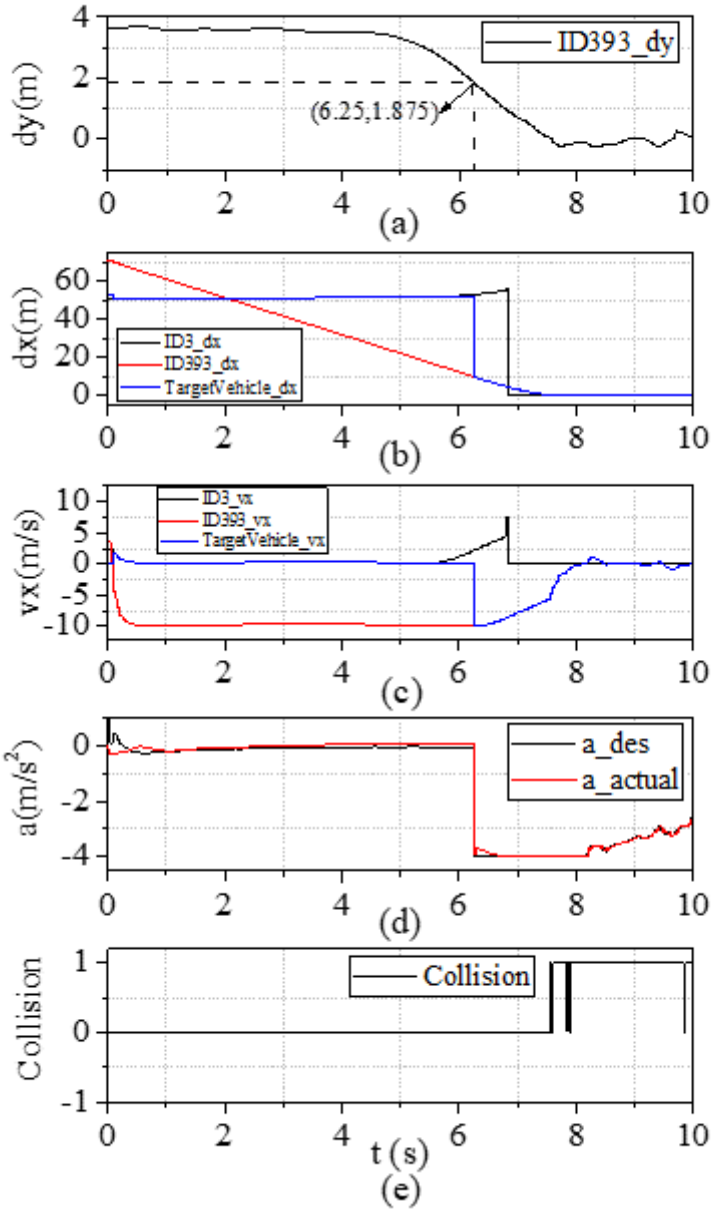

Figure 22

Simulation results of traditional ACC longitudinal control under dangerous lane-changing condition: (a) lateral relative distance of the preceding vehicle in the adjacent lane ID393; (b) relative longitudinal distance of the preceding vehicle in the current lane ID3, the preceding vehicle in the current lane ID393, the target vehicle; (c) relative longitudinal velocity of the preceding vehicle in the current lane ID3, the preceding vehicle in the current lane ID393, the target vehicle; (d) desired longitudinal acceleration and actual longitudinal acceleration of the subject vehicle; (e) collision during longitudinal control

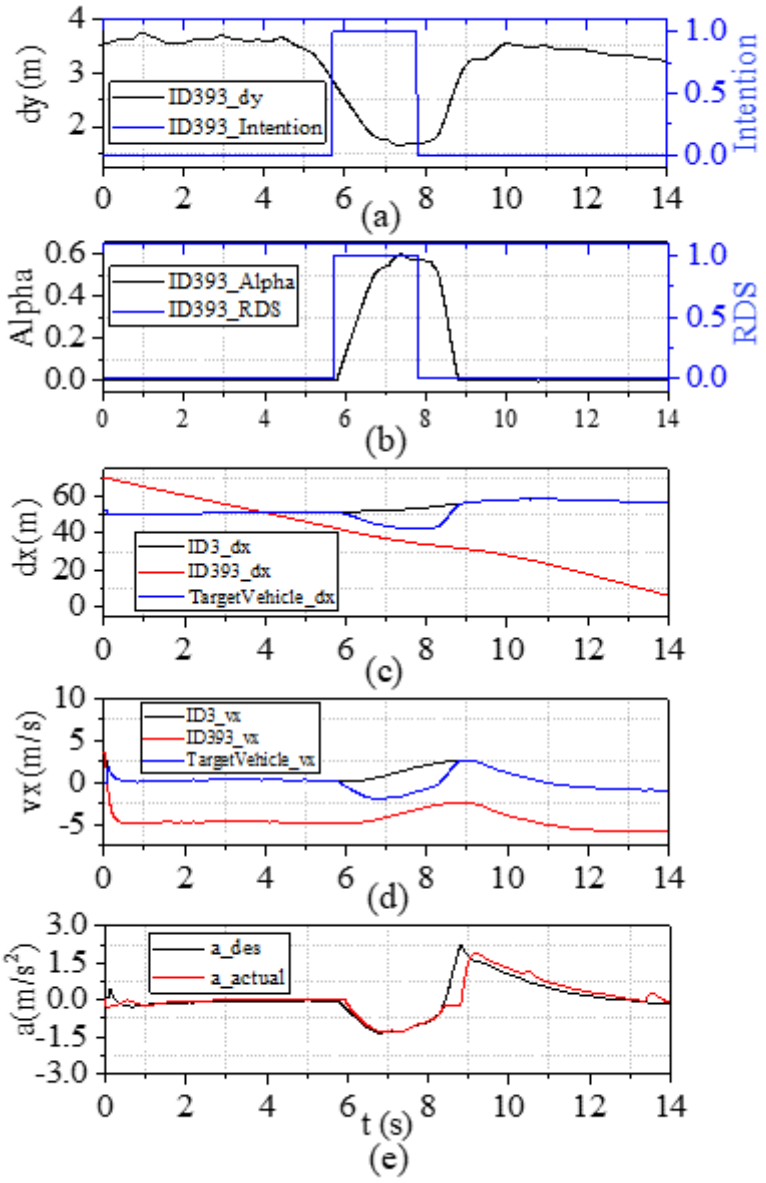

Figure 23

Simulation results of longitudinal control based on lane-changing intention prediction of preceding vehicle under lane-changing cancellation condition: (a) lateral relative distance and lane-changing intention of the preceding vehicle in the adjacent lane ID393; (b) α and RDS of the preceding vehicle in the adjacent lane ID393; (c) relative longitudinal distance of the preceding vehicle in the current lane ID3, the preceding vehicle in the current lane ID393, the target vehicle; (d) relative longitudinal velocity of the preceding vehicle in the current lane ID3, the preceding vehicle in the current lane ID393, the target vehicle; (e) desired longitudinal acceleration and actual longitudinal acceleration of the subject vehicle

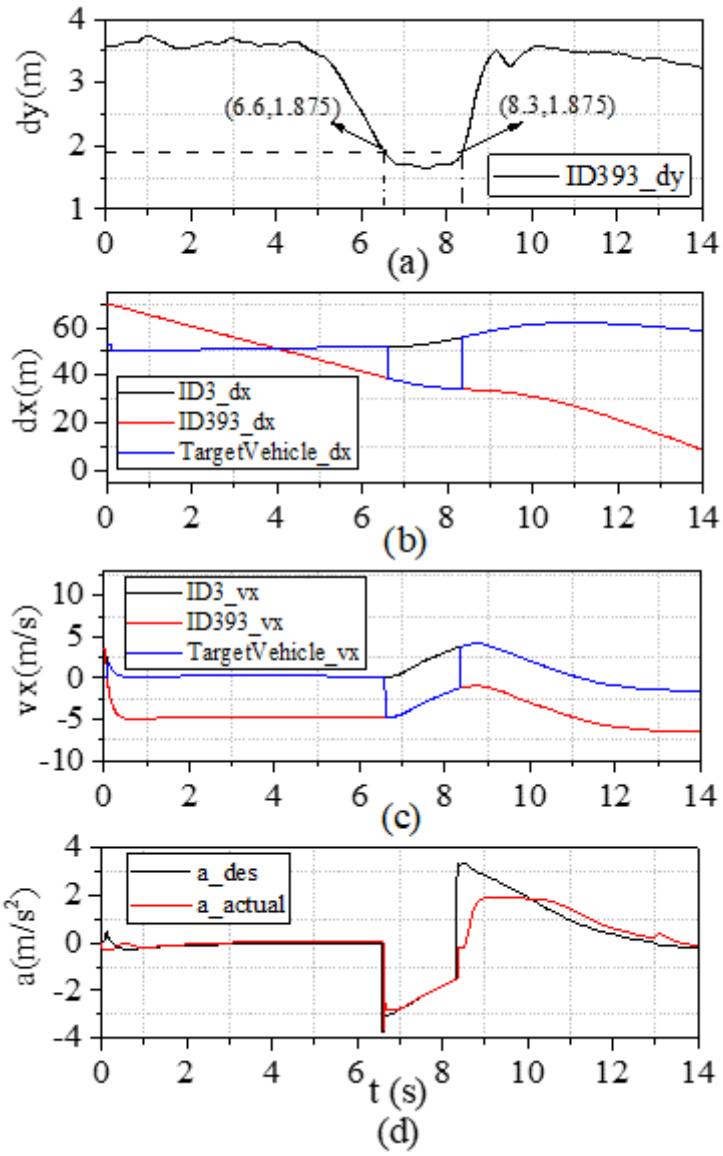

Figure 24

Simulation results of traditional ACC longitudinal control under lane-changing cancellation condition: (a) lateral relative distance of the preceding vehicle in the adjacent lane ID393; (b) relative longitudinal distance of the preceding vehicle in the current lane ID3, the preceding vehicle in the current lane ID393, the target vehicle; (c) relative longitudinal velocity of the preceding vehicle in the current lane ID3, the preceding vehicle in the current lane ID393, the target vehicle; (d) desired longitudinal acceleration and actual longitudinal acceleration of the subject vehicle